Unitarized pseudoscalar meson scattering amplitudes from three flavor linear sigma models

Deirdre Black,[1,*] Amir H. Fariborz,[2,†] Sherif Moussa,[1,‡] Salah Nasri,[1,§] and Joseph Schechter[1,‖]
[1]*Department of Physics, Syracuse University, Syracuse, New York 13244-1130*
[2]*Department of Mathematics/Science, State University of New York, Institute of Technology, Utica, New York 13504-3050*
(Received 20 December 2000; published 8 June 2001)

The three flavor linear sigma model is studied as a ''toy model'' for understanding the role of possible light scalar mesons in the $\pi\pi$, πK and $\pi\eta$ scattering channels. The approach involves computing the tree level partial wave amplitude for each channel and unitarizing by a simple K-matrix prescription which does not introduce any new parameters. If the renormalizable version of the model is used there is only one free parameter. While this highly constrained version has the right general structure to explain $\pi\pi$ scattering, it is ''not quite'' right. A reasonable fit can be made if the renormalizability (for the *effective* Lagrangian) is relaxed while chiral symmetry is maintained. The occurrence of a Ramsauer-Townsend mechanism for the $f_0(980)$ region naturally emerges. The effect of unitarization is very important and leads to ''physical'' masses for the scalar nonet all less than about 1 GeV. The $a_0(1450)$ and $K_0^*(1430)$ appear to be ''outsiders'' in this picture and to require additional fields. Comparison is made with a scattering treatment using a more general nonlinear sigma model approach. In addition some speculative remarks and a highly simplified larger toy model are devoted to the question of the quark substructure of the light scalar mesons.

DOI: 10.1103/PhysRevD.64.014031 PACS number(s): 13.75.Lb, 11.15.Pg, 11.80.Et, 12.39.Fe

I. INTRODUCTION

In the last few years there has been a revival of interest [1–27] in the possibility that light scalar mesons such as the sigma and kappa exist. This is a very important but highly controversial subject. The difficulty is that one must demonstrate their existence by comparing with experiment, believable theoretical amplitudes containing the light scalars. However, the energy range of interest is too low for the systematic perturbative QCD expansion and too high for the systematic chiral perturbation theory expansion [28]. Clearly, chiral symmetry should hold but it seems unavoidable to fall back on model dependent approaches. Qualitatively, the dominance of tree amplitudes is suggested by the $1/N_c$ expansion [29] and it has been shown by Schechter and co-workers [6,12,14,24] that this approach can be used to economically fit the data in the framework of a non-linear chiral Lagrangian which includes vectors and scalars in addition to the pseudoscalars. Many related approaches have been discussed by other workers [30]. To put the problem in historical perspective, the theoretical treatment of meson-meson scattering has been a topic of great interest for about forty years and has given rise, among other things, to chiral perturbation theory and string theory. Nevertheless, the problem itself of explaining light meson scattering amplitudes from threshold to (say) about the 1.5 GeV region is still not definitively solved. Of course, if the existence of light scalars is true, it will be a crucial step forward.

In such a situation, it is often useful to increase one's perspective by studying simplified ''toy models.'' The classic chiral symmetric model which contains a scalar meson is the Gell-Mann–Lévy two flavor linear sigma model [31]. At the tree level it yields essentially the same $\pi\pi$ scattering length which is the initial approximation in the chiral perturbation scheme. However, compared to that scheme, which uses a non-linear Lagrangian of pions only [32], it is less convenient to systematically implement corrections. Nevertheless it does contain a light scalar meson and it does provide the standard intuitive picture of spontaneous chiral symmetry breaking. Furthermore, it is likely to be [33] an accurate model close to the QCD chiral phase transition. Of course there is an enormous literature on the application of the two flavor linear sigma model to $\pi\pi$ scattering. Recently, Achasov and Shestakov [4] have shown that a qualitatively reasonable picture emerges at the lower part of our energy range of interest [34] by using a scheme which is equivalent to what we may call ''K-matrix unitarization.'' Namely, in the standard parametrization [35] of a given partial wave S matrix,

$$S=\frac{1+iK}{1-iK}\equiv 1+2iT, \tag{1.1}$$

we identify

$$K=T_{\text{tree}}. \tag{1.2}$$

T_{tree} is the given partial wave T matrix computed at tree level and is purely real. Such a scheme gives exact unitarity for T but violates the crossing symmetry which T_{tree} itself obeys.

For a more realistic application to $\pi\pi$ scattering [i.e. inclusion of the $f_0(980)$] as well as to πK, $\pi\eta$ scatterings etc. it is highly desirable to extend this calculation to the three flavor case. That is the purpose of this paper. We will see that it provides a very predictive and reasonably successful model which gives interesting new insights.

*Electronic address: black@physics.syr.edu
†Electronic address: fariboa@sunyit.edu
‡Electronic address: sherif@suhep.phy.syr.edu
§Electronic address: snasri@suhep.phy.syr.edu
‖Electronic address: schechte@suhep.phy.syr.edu

The three flavor linear sigma model [36] is constructed from the 3×3 matrix field

$$M=S+i\phi \tag{1.3}$$

where $S=S^\dagger$ represents a scalar nonet and $\phi=\phi^\dagger$ a pseudoscalar nonet. Under a chiral transformation $q_L\to U_L q_L$, $q_R\to U_R q_R$ of the fundamental left and right handed light quark fields, M is defined to transform as

$$M\to U_L M U_R^\dagger. \tag{1.4}$$

To start with, one may consider a general non-renormalizable [37] Lagrangian of the form

$$\mathcal{L}=-\frac{1}{2}\mathrm{Tr}(\partial_\mu\phi\partial_\mu\phi)-\frac{1}{2}\mathrm{Tr}(\partial_\mu S\partial_\mu S)-V_0-V_{SB}, \tag{1.5}$$

where V_0 is an arbitrary function of the independent $SU(3)_L\times SU(3)_R\times U(1)_V$ invariants

$$I_1=\mathrm{Tr}(MM^\dagger),\quad I_2=\mathrm{Tr}(MM^\dagger MM^\dagger),$$
$$I_3=\mathrm{Tr}((MM^\dagger)^3),\quad I_4=6(\det M+\det M^\dagger). \tag{1.6}$$

Of these, only I_4 is not invariant under $U(1)_A$. The symmetry breaker V_{SB} has the minimal form

$$V_{SB}=-2(A_1S_1^1+A_2S_2^2+A_3S_3^3), \tag{1.7}$$

where the A_a are real numbers which turn out to be proportional to the three light (''current'' type) quark masses.

The Lagrangian Eq. (1.5) contains the most general ''potential'' term V_0 but still has the minimal ''kinetic'' term. It is possible[1] to also include non-renormalizable kinetic-type terms like $\mathrm{Tr}(\partial_\mu M\partial_\mu M^\dagger MM^\dagger)$, $\mathrm{Tr}(\partial_\mu MM^\dagger\partial_\mu MM^\dagger)$ +H.c., etc. We shall disregard such terms in the present paper. It is interesting to note [37] that the results of ''current algebra'' can be derived from Eq. (1.5) without knowing details of V_0, just from chiral symmetry and the assumption that the minimum of $V\equiv V_0+V_{SB}$ is non-zero; specifically the ''vacuum values'' satisfy

$$\langle S_a^b\rangle=\alpha_a\delta_a^b. \tag{1.8}$$

The ''one-point'' vertices (pseudoscalar decay constants) are related to these parameters by

$$F_\pi=\alpha_1+\alpha_2,\quad F_K=\alpha_1+\alpha_3. \tag{1.9}$$

In the isotopic spin invariant limit one has

$$A_1=A_2,\quad \alpha_1=\alpha_2\ \ (\text{isospin limit}). \tag{1.10}$$

Many, though not all, of the ''two-point'' vertices (particle squared masses) may be calculated by [37] single differentiation of two ''generating equations'' which express the chiral symmetry of V_0 and also using

$$\left\langle\frac{\partial V}{\partial S_a^b}\right\rangle=0. \tag{1.11}$$

For example, one finds

$$m^2(\pi^+)=2\frac{A_1+A_2}{\alpha_1+\alpha_2},\quad m^2(K^+)=2\frac{A_1+A_3}{\alpha_1+\alpha_3}. \tag{1.12}$$

The formula for the mass of the η' (and of the particles η and π^0 with which it may mix) also involves the quantity

$$V_4\equiv\left\langle\frac{\partial V_0}{\partial I_4}\right\rangle. \tag{1.13}$$

Many of the three point and four point vertices may be obtained by respectively two times and three times differentiating the above mentioned generating equations. The specific terms needed for our subsequent discussion are given in the Appendix.

The present model requires us (in the limit of isospin invariance) to specify the five parameters, A_1, A_3, α_1, α_3 and V_4. These may be obtained by using the five experimental input values:

$$m_\pi=0.137\ \text{GeV},\quad m_K=0.495\ \text{GeV},$$
$$m_\eta=0.457\ \text{GeV},\quad m_{\eta'}=0.958\ \text{GeV},$$
$$F_\pi=0.131\ \text{GeV}\quad(\text{inputs}). \tag{1.14}$$

This is a reasonable, but clearly not unique choice for the inputs. (For example, F_K might be used instead of m_η.) With these input parameters there are two immediate predictions for pseudoscalar properties:

$$\theta_p=2.05^\circ,\quad \frac{F_K}{F_\pi}=1.39, \tag{1.15}$$

where the pseudoscalar mixing angle, θ_p, is here defined by

$$\begin{pmatrix}\eta\\ \eta'\end{pmatrix}=\begin{pmatrix}\cos\theta_p & -\sin\theta_p\\ \sin\theta_p & \cos\theta_p\end{pmatrix}\begin{pmatrix}\eta_8\\ \eta_0\end{pmatrix}. \tag{1.16}$$

η and η' are the ''physical'' states while the ''unmixed'' states are $\eta_8=(\phi_1^1+\phi_2^2-2\phi_3^3)/\sqrt{6}$ and $\eta_0=(\phi_1^1+\phi_2^2+\phi_3^3)/\sqrt{3}$. The predictions in Eq. (1.15) are qualitatively reasonable but not very accurate; the usually accepted value for θ_p, while small, is [39] around -18° and the experimental value for F_K/F_π is about 1.22. (It is likely that the inclusion of non-renormalizable kinetic terms mentioned above will improve this aspect.)

Now, the scalar meson masses are of the most present interest. Analogously to the pseudoscalars (π, K, η_0, η_8) we denote the scalars by (a_0, κ, σ_0, σ_8). The predicted squared masses from the ''toy'' Lagrangian in Eq. (1.5) are

$$(\alpha_2-\alpha_1)m^2_{\mathrm{BARE}}(a_0^+)=2(A_2-A_1),$$

[1]See, for example, Sec. IV of [38].

$$m^2_{\rm BARE}(\kappa^+)=\frac{2(A_3-A_1)}{\alpha_3-\alpha_1},$$

$$m^2_{\rm BARE}(\kappa^0)=\frac{2(A_3-A_2)}{\alpha_3-\alpha_2}. \qquad (1.17)$$

In this case, the masses of σ_0, σ_8 and their mixing angle θ_s [defined analogously to Eq. (1.16)] are *not* predicted. In the isotopic spin invariant limit, which we shall adopt here, the a_0 mass is not predicted (although it may be reasonably estimated [40] by taking isospin violation into account). Note that we have, in contrast to the pseudoscalar case, put a subscript ''BARE'' on each scalar mass. This is because the pole positions in the pseudoscalar-pseudoscalar scattering amplitudes corresponding to scalar mesons may be nontrivially shifted by the unitarization procedure of Eqs. (1.1) and (1.2). We consider the unitarization to be an approximation to including all higher order corrections. Then, in the usual field theoretic way of thinking, the pole position determines the physical mass, while the tree level $m_{\rm BARE}$ has no clear physical meaning.

The tree level $\pi\pi$ scattering amplitude is easily computed [37] from Eq. (1.5) in the present scheme. It involves a four point ''contact'' amplitude and σ and σ' exchange diagrams. The resulting form[2] turns out to be remarkably simple:

$$A(s,t,u)=\frac{2}{F_\pi^2}\left\{ m_\pi^2+\cos^2\psi\left[\frac{(m^2_{\rm BARE}(\sigma)-m_\pi^2)^2}{m^2_{\rm BARE}(\sigma)-s}-m^2_{\rm BARE}(\sigma)\right]+\sin^2\psi\left[\frac{(m^2_{\rm BARE}(\sigma')-m_\pi^2)^2}{m^2_{\rm BARE}(\sigma')-s}-m^2_{\rm BARE}(\sigma')\right]\right\}, \qquad (1.18)$$

where s, t and u are the usual Mandelstam variables. The angle ψ is defined by the transformation

$$\begin{pmatrix}\sigma\\ \sigma'\end{pmatrix}=\begin{pmatrix}\cos\psi & -\sin\psi\\ \sin\psi & \cos\psi\end{pmatrix}\begin{pmatrix}\frac{S_1^1+S_2^2}{\sqrt{2}}\\ S_3^3\end{pmatrix}, \qquad (1.19)$$

where[3] ψ is related to the angle θ_s [defined analogously to Eq. (1.16)] by

$$\cos\psi=\frac{1}{\sqrt{3}}(\cos\theta_s-\sqrt{2}\sin\theta_s), \qquad (1.20)$$

which translates to $\psi\approx\theta_s+54.7°$. With the Lagrangian Eq. (1.5) the amplitude Eq. (1.18) depends on the three unknown parameters $m_{\rm BARE}(\sigma)$, $m_{\rm BARE}(\sigma')$ and ψ.

We can increase the predictivity of the model by restricting the potential V_0 in Eq. (1.5) to contain only renormalizable terms. The resulting model is the one usually considered since it allows for a consistent perturbation treatment (although the coupling constants are very large). In any event, we will be working at tree level and ''simulating'' higher order corrections by the K-matrix unitarization procedure. Note that all the formulas gotten above with general V_0 continue to hold in the renormalizable model; there will just be additional restrictions. The renormalizable potential may be written [41] as

$$V_0(\text{renormalizable})=[V_1-V_{11}(\Sigma_a\alpha_a^2)]I_1+\frac{1}{2}V_{11}(I_1)^2+V_2I_2+V_4I_4, \qquad (1.21)$$

where we have used the notation

$$V_a\equiv\left\langle\frac{\partial V_0}{\partial I_a}\right\rangle,\quad V_{ab}\equiv\left\langle\frac{\partial^2 V_0}{\partial I_a\partial I_b}\right\rangle. \qquad (1.22)$$

As discussed[4] in [41], we may determine V_1 and V_2 from the extremum equation Eq. (1.11) while V_{11} may be expressed in terms of $m_{\rm BARE}(\sigma)$. Thus specifying $m_{\rm BARE}(\sigma)$ determines the model parameters completely. Actually, $m_{\rm BARE}(a_0)$ is fixed to be 0.913 GeV just by requiring renormalizability, independent of the choice of $m_{\rm BARE}(\sigma)$. Using Eq. (1.17) we find that $m_{\rm BARE}(\kappa)=0.909$ GeV, independent of whether we make the renormalizability restriction or not. Finally, the dependences of $m_{\rm BARE}(\sigma')$ and θ_s on the choice of $m_{\rm BARE}(\sigma)$ are displayed in Fig. 1. Choosing the convention where $m_{\rm BARE}(\sigma)<m_{\rm BARE}(\sigma')$, the model does not allow for $m_{\rm BARE}(\sigma)$ greater than about 0.813 GeV. Furthermore $m_{\rm BARE}(\sigma')$ must be greater than about 0.949 GeV in the renormalizable model.

In Sec. II we study the simpler two flavor model both for the purpose of review and for introducing our notation and the method we will use in the three flavor case. We will also illustrate just how well the amplitude can be approximated by a pole in the complex s-plane plus a constant. A number of new remarks are made. Section III contains a detailed discussion of the s-wave $\pi\pi$, πK and $\pi\eta$ scattering amplitudes in the unitarized three flavor model. Both plots of the predicted amplitudes compared with experiment and numerical calculation of the pole parameters will be seen to be useful for understanding the dynamics. A summary and discussion of the calculations of the scalar meson parameters are presented in Sec. IV. Section V contains a more specu-

[2]The sign of $A(s,t,u)$ is the negative of the one in the convention of [37] but in agreement with those in [12,13,23].

[3]Note that neither ψ nor θ_s are defined in the same way as θ_s in Eq. (3.6) of [15].

[4]Please notice the relevant typographical errors in [41]: (1) In the first of Eqs. (2.2), $A_3/w-1$ should be replaced by $A_3/w-A_1$. (2) In the second line of Eq. (2.5c) $4\alpha w V_{11}$ should be replaced by $4\alpha^2 w V_{11}$. (3) In the numerator of Eq. (2.8) the factor $(4\alpha)^{-2}$ should be replaced by $(2\alpha)^{-2}$.

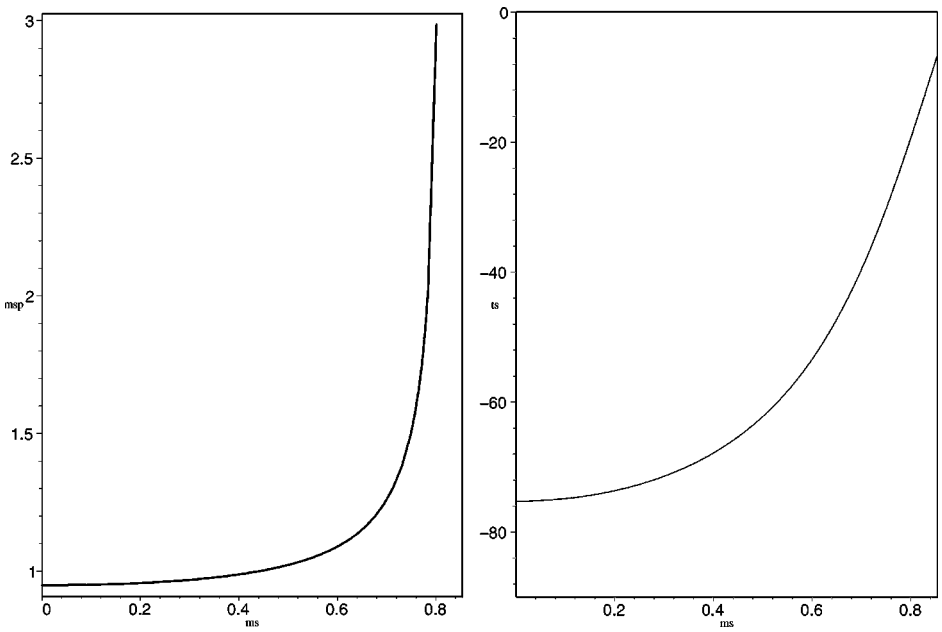

FIG. 1. Dependence (left) of $m_{\mathrm{BARE}}(\sigma')$ in GeV and (right) of the octet-singlet mixing angle θ_s in degrees on $m_{\mathrm{BARE}}(\sigma)$, in the renormalizable linear sigma model.

lative discussion on the question of the ''quark substructure'' of the light scalars. It is pointed out that there is a difference in describing this at the ''current'' and ''constituent'' quark levels. Also, while the linear sigma model is set up on the ''current'' quark basis, it does not uniquely describe the quark substructure. In the present model, the initial ''current-quark'' meson field leads to constituent type states which are modified both by details of symmetry breaking and by unitarization. The possible richness of the scalar meson system for further study is illustrated by the introduction of a larger toy model which includes two different M matrices.

II. TWO FLAVOR LINEAR SIGMA MODEL

It seems useful to first review the two flavor case and to make some additional comments. We start by exploring the difficulty with a conventional extension of the tree level amplitude beyond the threshold region. This also provides the usual motivation for the introduction of the nonlinear sigma model.

A. Standard unitarization procedure and its problems

It is easy to get the two flavor $\pi\pi$ scattering amplitude by taking a suitable limit of the three flavor amplitude given in Eq. (1.18). We simply decouple the σ' by setting the $\sigma - \sigma'$ mixing angle ψ to zero, as is evident in Eq. (1.19). Then σ becomes $(S_1^1+S_2^2)/\sqrt{2}$, while $\sigma'=S_3^3$ does not belong to the SU(2) theory and decouples; we are left with the tree amplitude:[5]

$$A(s,t,u)=\frac{2}{F_\pi^2}[m^2_{\mathrm{BARE}}(\sigma)-m_\pi^2]\left[\frac{m^2_{\mathrm{BARE}}(\sigma)-m_\pi^2}{m^2_{\mathrm{BARE}}(\sigma)-s}-1\right]. \tag{2.1}$$

The pole term in the second bracket represents the σ exchange Feynman diagram. Naively one would expect this term by itself to describe σ dominance of the low energy amplitude. However, the (-1) piece, which comes from the four point contact interaction, is needed in this model to satisfy chiral symmetry. It is easy to see that there is a dramatic partial cancellation of the two terms near threshold. For example, if we take the single unknown parameter in the model, $m_{\mathrm{BARE}}(\sigma)$ to be 1 GeV, then the pole term at threshold $[s_{th}=4m_\pi^2]$ is about 1.06. This gets reduced to just 6% of its value after adding the constant piece. Near threshold we can approximate $m^2_{\mathrm{BARE}}(\sigma)\gg[m_\pi^2,s]$ to get the famous ''current algebra'' [42] formula

$$A(s,t,u)\approx\frac{2(s-m_\pi^2)}{F_\pi^2}. \tag{2.2}$$

We have just seen that this is a small quantity which has arisen from a partial cancellation of two relatively large terms. Now if we wish to use Eq. (2.1) away from threshold we run into the problem of an infinity arising when $s=m^2_{\mathrm{BARE}}(\sigma)$. A standard unitarization procedure to avoid this problem would correspond to making the replacement

$$\frac{1}{m^2_{\mathrm{BARE}}(\sigma)-s}\to\frac{1}{m^2_{\mathrm{BARE}}(\sigma)-s-i\Gamma m_{\mathrm{BARE}}(\sigma)}, \tag{2.3}$$

where Γ is a width factor. The trouble is that the delicate partial cancellation with the contact term is now spoiled near threshold and consequently there will be a very poor agreement with experiment in the threshold region.

[5]Since this formula was gotten as a limit of the SU(3) model with an arbitrary (not neccessarily a fourth order polynomial) potential, we see that the tree result Eq. (2.1) is independent of whether the SU(2) linear sigma model potential has only renormalizable terms.

The most popular alternative treatment introduces a non-linearly transforming pion field and no σ at all. (Formally it may be gotten by ''integrating out'' the σ of the linear model but this is not the most general formulation.) Then the current algebra formula Eq. (2.2) is obtained directly from a derivative type four point contact term (as opposed to the non-derivative type in the linear model). This approach forms the basis of the chiral perturbation scheme (of pions only). The next order correction will involve more powers of derivatives and hence will not drastically modify the already reasonable current algebra result.

A sigma-type particle can be introduced in a general way (independent of the linear sigma model) in the non-linear framework by using a standard technique [43]. In this approach the $\sigma\pi\pi$ couplings are inevitably of derivative type so the σ-pole contribution is small near threshold and does not drastically alter the current algebra result. This is clearly convenient since a regularization of the type Eq. (2.3) will not now alter the threshold behavior drastically. However, this does not neccessarily guarantee good experimental agreement away from threshold.

It seems worthwhile to emphasize that general models made using either linearly or non-linearly transforming chiral fields represent the same physics—spontaneous breakdown of chiral symmetry. The choice of which to use is hence primarily a question of convenience in extending the description away from threshold. Usually the non-linear approach is a lot more convenient. In this paper we focus on studying the linear model, regarding it as a ''toy model'' useful for increasing our understanding.

To go further, we need the partial wave projection of the amplitude Eq. (2.1). Here we specialize to the I=0 projection:

$$A^{\mathrm{I}=0}=3A(s,t,u)+A(u,t,s)+A(t,s,u). \tag{2.4}$$

The angular momentum l partial wave elastic scattering amplitude for isospin I is

$$T_l^I(s)=\frac{1}{2}\rho(s)\int_{-1}^{1} d\cos\theta\, P_l(\cos\theta)A^I(s,t,u), \tag{2.5}$$

where $A^I(s,t,u)$ is the isospin I invariant amplitude, θ is the center of mass scattering angle and

$$\rho(s)=\frac{q(s)}{16\pi\sqrt{s}}, \tag{2.6}$$

with $q(s)$ the center of mass momentum for, in general, a channel containing particles a_1 and a_2:

$$q^2=\frac{s^2+(m_{a_1}^2-m_{a_2}^2)^2-2s(m_{a_1}^2+m_{a_2}^2)}{4s}. \tag{2.7}$$

T_l^I is related to the partial wave S-matrix, S_I^l by Eq. (1.1). For understanding the properties of the σ-meson, the T_0^0 amplitude is clearly the most relevant. Using Eq. (2.1) and Eqs. (2.4)–(2.7) we get the tree approximation

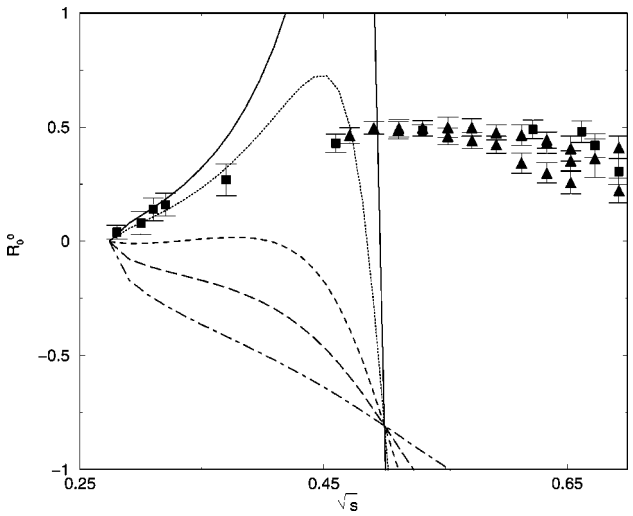

FIG. 2. Predicted real part of $\pi\pi$ I=0 s-wave amplitude using regularization with different constant widths according to Eq. (2.3). The widths are 50 MeV (solid), 100 MeV (dots), 200 MeV (dashes), 300 MeV (long-dashes), 500 MeV (dot-dashes). Here, $m_{\mathrm{BARE}}(\sigma)=560$ MeV.

$$T_{0tree}^0(s)=\alpha(s)+\frac{\beta(s)}{m_{\mathrm{BARE}}^2(\sigma)-s} \tag{2.8}$$

where

$$\alpha(s)=\rho(s)\frac{m_{\mathrm{BARE}}^2(\sigma)-m_\pi^2}{F_\pi^2}\left[-10+4\frac{m_{\mathrm{BARE}}^2(\sigma)-m_\pi^2}{s-4m_\pi^2}\times\ln\left(\frac{m_{\mathrm{BARE}}^2(\sigma)+s-4m_\pi^2}{m_{\mathrm{BARE}}^2(\sigma)}\right)\right],$$

$$\beta(s)=\frac{6\rho(s)}{F_\pi^2}(m_{\mathrm{BARE}}^2(\sigma)-m_\pi^2)^2. \tag{2.9}$$

Note that $\alpha(s)$ in Eq. (2.9) does *not* blow up when $q^2=(s-4m_\pi^2)/4\to 0$.

Using the partial wave amplitude Eqs. (2.8) and (2.9) it is straightforward to give a more detailed discussion of the difficulty of regulating the infinity at $s=m_{\mathrm{BARE}}^2(\sigma)$ while still maintaining the good agreement near threshold. Consider replacing the denominator in Eq. (2.8) according to the prescription Eq. (2.3). The effect of different constant widths Γ in Eq. (2.3) is illustrated in Fig. 2 for an arbitrary choice of $m_{\mathrm{BARE}}(\sigma)=560$ MeV. It is seen that the effect of increasing the width is to change the slope of the real part of $T_0^0(s)$, $R_0^0(s)$ near threshold from positive to negative, which contradicts experiment [44]. Note that the unitarity bound $|R_0^0(s)|\leqslant\frac{1}{2}$ is violated not too far away from threshold. Theoretically, it is most natural to use instead of an arbitrary constant, the ''running'' perturbative width,

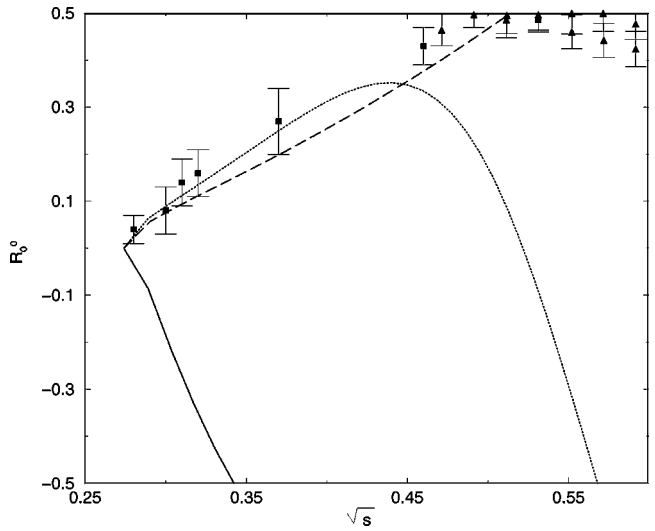

FIG. 3. Variations on SU(2) linear sigma model prediction for real part of $\pi\pi$ I=0 s-wave amplitude. The dashed curve is the ''current algebra'' result Eq. (2.2), the solid curve uses Eq. (2.3) with the perturbative width calculated from Eq. (2.10) and the dotted curve uses the regularization prescription outlined around Eq. (2.11). Here, $m_{\rm BARE}(\sigma)=560$ GeV.

$$\Gamma(s)=\frac{3}{16\pi F_\pi^2\sqrt{s}}\sqrt{1-\frac{4m_\pi^2}{s}}[m_{\rm BARE}^2(\sigma)-m_\pi^2]^2, \tag{2.10}$$

as was tried also in [4]. A plot of the real part of the resulting amplitude $R_0^0(s)$ is shown in Fig. 3 and is seen to badly disagree with experiment. This is due to the large value of the perturbative width $\Gamma[s=m_{\rm BARE}^2(\sigma)]$. It is amusing that the somewhat arbitrary modification in the last factor of Eq. (2.10):

$$[m_{\rm BARE}^2(\sigma)-m_\pi^2]^2\to[s-m_\pi^2]^2 \tag{2.11}$$

greatly improves the agreement near threshold, as is also shown in Fig. 3. However somewhat beyond threshold the amplitude also starts to deviate greatly from experiment. Thus the prescription Eq. (2.11) does not completely solve the problem, but may help fitting to experiment if the effects of other possible particles are also taken into account. The effect of different values of $m_{\rm BARE}(\sigma)$ in Eq. (2.9) is illustrated in Fig. 4 for this scheme.

B. *K*-matrix unitarization

We can force unitarity at all s for the scalar partial wave amplitude, $T_0^0(s)$ by taking the tree amplitude $T_{0\rm tree}^0(s)$ given in Eqs. (2.8) and (2.9) to coincide with $K(s)$ in Eq. (1.1). To see what is happening first consider $T_{0\rm tree}^0(s)$ to be small (for example near the $\pi\pi$ scattering threshold). Then, in this single channel case,

$$S_0^0\equiv 1+2iT_0^0=1+2iT_{0\rm tree}^0(s)+\cdots, \tag{2.12}$$

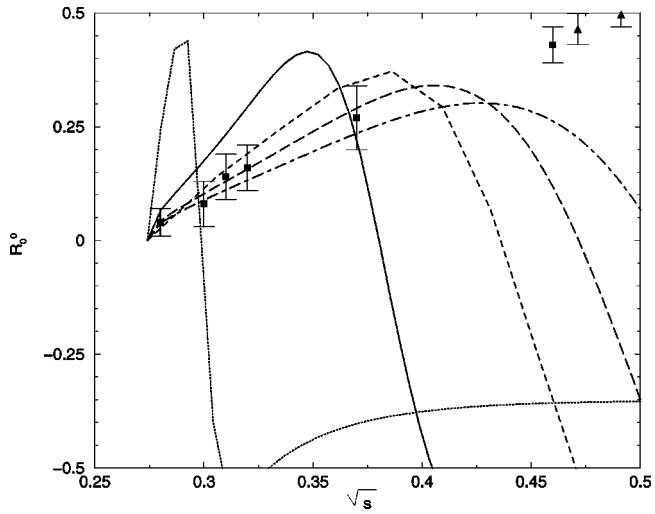

FIG. 4. Effect of different values of $m_{\rm BARE}(\sigma)$ on the generalized ''running width'' prescription, outlined around Eq. (2.11), on the SU(2) linear sigma model prediction for real part of the $\pi\pi$ I=0 s-wave scattering amplitude. We show the curves for (in MeV) $m_{\rm BARE}(\sigma)=300$ (dots), 400 (solid), 500 (dashes), 600 (long dashes) and 800 (dot-dashes).

so that $T_0^0(s)$ starts out as $T_{0\rm tree}^0(s)$, which is a reasonable approximation. A presumably better approximation is obtained by including more terms in an expansion of the denominator:

$$T_0^0(s)=\frac{T_{0\rm tree}^0}{1-iT_{0\rm tree}^0}=T_{0\rm tree}^0[1+iT_{0\rm tree}^0+(iT_{0\rm tree}^0)^2+\cdots]. \tag{2.13}$$

As observed in [4] this has the structure of a bubble sum in field theory. However, in the present case one is working with the partial wave, rather than the invariant amplitude so there is no integration over intermediate state momenta. Of course, in either case, crossing symmetry is lost. While $T_{0\rm tree}^0$ is gotten from a crossing symmetric invariant amplitude, it is unlikely that the specially iterated amplitude Eq. (2.13) can be gotten in this way. The advantage of the method is that it guarantees unitarity. If, as is common, $T_{0\rm tree}^0(s)$ starts getting too large, T_0^0 will be chopped down to size. For example if $T_{0\rm tree}^0$ gets very large:

$$S_0^0\to -1; \quad T_0^0\to i. \tag{2.14}$$

The real part R_0^0 of T_0^0 vanishes in such a case while the imaginary part $I_0^0\to 1$. In particular this occurs, as we see from Eq. (2.8), at the pole of $T_{0\rm tree}^0$, where $s=m_{\rm BARE}^2$.

With the tree level amplitude of Eq. (2.8), the unitarized S-matrix takes the form

$$S_0^0(s)=\frac{[1+i\alpha(s)][m_{\rm BARE}^2(\sigma)-s]+i\beta(s)}{[1-i\alpha(s)][m_{\rm BARE}^2(\sigma)-s]-i\beta(s)}, \tag{2.15}$$

where $\alpha(s)$ and $\beta(s)$ are given in Eq. (2.9). Equation (2.15) is sufficient for comparing the predictions of the model

[which contains the single unknown parameter $m_{\mathrm{BARE}}(\sigma)$] with the experiment. However it is also of interest to rewrite the amplitude so that it looks more like a conventional resonance in the presence of a background. Manipulating Eq. (2.15) gives the factorized expression

$$S_0^0(s)=e^{2i\delta_{bg}(s)}\frac{m'^2(s)-s+i\beta'(s)}{m'^2(s)-s-i\beta'(s)}, \tag{2.16}$$

where

$$\tan[\delta_{bg}(s)]=\alpha(s),$$

$$m'^2(s)=m_{\mathrm{BARE}}^2(\sigma)+\frac{\alpha(s)\beta(s)}{1+\alpha^2(s)},$$

$$\beta'(s)=\frac{\beta(s)}{1+\alpha^2(s)}. \tag{2.17}$$

This has the desired form although it should be noted that m' and β' are both s-dependent. The T amplitude which follows from Eq. (2.16) and Eq. (1.1) is the sum of a background term and a modified resonance term

$$T_0^0(s)=e^{i\delta_{bg}(s)}[\sin\delta_{bg}(s)]+e^{2i\delta_{bg}(s)}\frac{\beta'(s)}{m'^2-s-i\beta'(s)}. \tag{2.18}$$

It is important to observe that the resonance mass and width (corresponding to a pole in the complex s plane) are shifted from their bare values. These new values should be obtained from the complex solution,[6] z_σ of

$$m'^2(z)-z-i\beta'(z)=0. \tag{2.19}$$

We may choose to identify the *physical* mass and width of the σ from[7]

$$m_\sigma^2-im_\sigma\Gamma_\sigma=z_\sigma. \tag{2.20}$$

One should keep in mind that the resonance term is no longer precisely of Breit-Wigner form.

A plot of the real part $R_0^0(s)$ of Eq. (2.18) is presented in Fig. 5 for the choices of (the single parameter in the model) $m_{\mathrm{BARE}}(\sigma)=0.5$ GeV, 0.8 GeV and 1 GeV. It is seen, as already noted in [4], that there is reasonable agreement with experiment up to about $\sqrt{s}=0.8$ GeV if $m_{\mathrm{BARE}}(\sigma)$ lies in the 0.8 to 1 GeV range. Beyond $\sqrt{s}=0.8$ GeV, the effects of the $f_0(980)$, which does not appear in the two flavor model, are clearly important. Also, the unitarized curves for $m_{\mathrm{BARE}}(\sigma)$ in the 0.8 to 1 GeV range give a reasonable looking description of the threshold region, as opposed to the conventional unitarization scheme of Eq. (2.3).

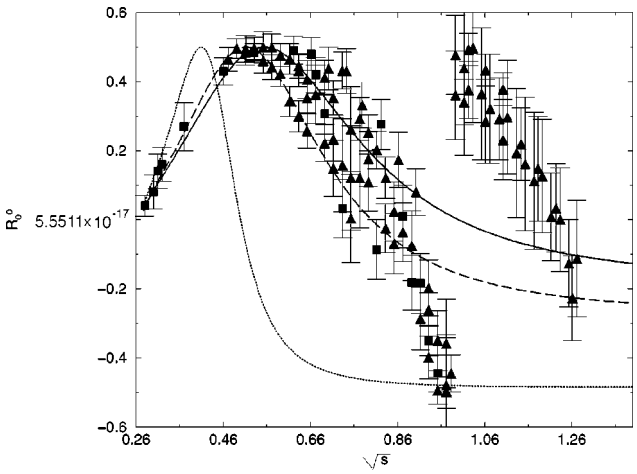

FIG. 5. Comparison with experiment of real part of the I=J=0 $\pi\pi$ scattering amplitude in the SU(2) linear sigma model, for $m_{\mathrm{BARE}}(\sigma)=0.5$ GeV (dots), $m_{\mathrm{BARE}}(\sigma)=0.8$ GeV (dashes) and $m_{\mathrm{BARE}}(\sigma)=1$ GeV (solid). Experimental data [44] are extracted from Alekseeva *et al.* (squares) and Grayer *et al.* (triangles).

Figure 6 shows how the K matrix unitarization works in detail by comparing $R_0^0(s)$ with $R_0^0(s)_{tree}$. It is seen that R_{0tree}^0 already violates the unitarity bound at $\sqrt{s}=0.43$ GeV.

Since we are regarding the K-matrix unitarization as a method of approximating all the higher order corrections to the $\pi\pi$ scattering amplitude, it is clear that the quantities of physical significance should not be the bare mass and width of σ but rather the pole mass m_σ and width Γ_σ defined (with a usual convention) by Eqs. (2.19) and (2.20). These quantities were obtained numerically and are given in Table I for the three choices of $m_{\mathrm{BARE}}(\sigma)$ used above. Evidently there

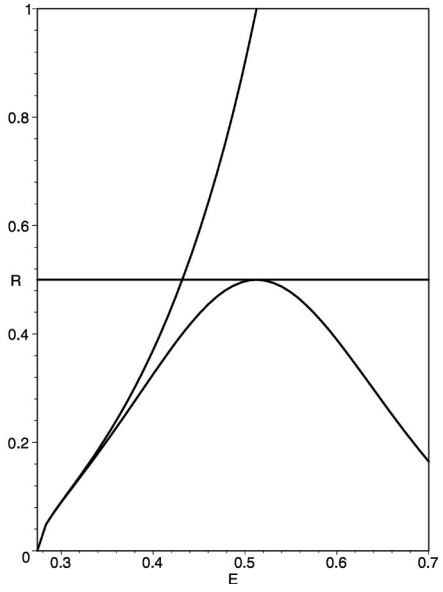

FIG. 6. Comparison of real part of K-matrix regularized I=J=0 $\pi\pi$ scattering amplitude with the diverging real part of the tree approximation, for $m_{\mathrm{BARE}}(\sigma)=0.8$ GeV.

[6]For complex arguments the ln function in $\alpha(z)$ is chosen to have an imaginary piece lying between $-i\pi$ and $i\pi$.

[7]A different definition of the resonance mass and width was used in [4] but the numerical results are close to each other.

TABLE I. Physical σ parameters in the two flavor linear sigma model.

$m_{\mathrm{BARE}}(\sigma)$ (GeV)	0.5	0.8	1
$\Gamma_{\mathrm{BARE}}(\sigma)$ (GeV)	0.311	1.58	3.22
m_σ (GeV)	0.421	0.458	0.449
Γ_σ (GeV)	0.202	0.476	0.624
z_σ (GeV^2)	$0.177-0.085$ i	$0.210-0.218$ i	$0.202-0.281$ i
a_σ (GeV^2)	$-0.015+0.078$ i	$0.088+0.169$ i	$0.158+0.188$ i
b_σ	$-0.420+0.443$ i	$-0.324+0.704$ i	$-0.274+0.753$ i

are very substantial shifts of the bare mass and the bare width. The physical sigma pole mass is around 0.45 GeV while the pole width is around 0.5–0.6 GeV for $m_{\mathrm{BARE}}(\sigma)$ in the 0.8 to 1 GeV range.

In the present model we may qualitatively understand the decrease in the σ mass and also width by noting that $\alpha(s)$ and $\beta(s)$ vary slowly with s. If they are taken to be constant the physical mass m_σ would coincide with m' in Eq. (2.17) and the physical quantity $m_\sigma\Gamma_\sigma$ with β' in Eq. (2.17). Thus the negative sign of the mass shift arises since the background piece of the amplitude $\alpha(s)$ is negative. A rather rough estimate may be made by evaluating $\alpha(s)$ and $\beta(s)$ for $m_\pi=0$ and s small. Then one finds $\beta \rightarrow 3m^4_{\mathrm{BARE}}(\sigma)/16\pi \mathrm{F}^2_\pi$ while $\alpha\rightarrow -\beta/m^2_{\mathrm{BARE}}(\sigma)$.

It is interesting to note that our calculated amplitude $T^0_0(s)$ can be reasonably well-approximated as

$$T^0_0(s)=\frac{a_\sigma}{s-z_\sigma}+b_\sigma, \tag{2.21}$$

where the two complex numbers a and b are given in Table I for different choices of $m_{\mathrm{BARE}}(\sigma)$. Since this simple pole dominated form reasonably fits experiment until the 700–800 MeV range it is not surprising that various determinations of m_σ and Γ_σ in the literature are roughly similar to the ones in Table I. Often the σ parameters are stated in terms of $z^{1/2}$. In the case where $m_\sigma=0.458$ GeV we have $z^{1/2}=0.517-i0.240$ GeV. This may be compared, for example, with a treatment using a non-linear sigma model and including the ρ meson [12]. That treatment gave a best fit for $z^{1/2}=0.585-i0.170$ GeV. When it was refit [13] without the ρ it yielded $z^{1/2}=0.493-i0.319$ GeV, which is closer to the value in the present study (wherein, of course, spin 1 particles have not been included).

III. SCATTERING IN THREE FLAVOR LINEAR SIGMA MODELS

Here we study the pseudoscalar meson scattering amplitudes in the three flavor linear sigma models discussed in the Introduction. We shall restrict attention to the J=0 elastic scattering amplitudes of

$$\pi\pi\rightarrow\pi\pi,$$

$$\pi K\rightarrow\pi K,$$

$$\pi\eta\rightarrow\pi\eta, \tag{3.1}$$

which contain the scalars of the model - (a_0, κ, σ, σ') - in the direct channel.

Exactly the same K-matrix unitarization scheme of Eqs. (1.1) and (1.2) which was used in the two flavor model will be employed. In particular, no special assumptions about the interplay of the σ and σ' resonances in $\pi\pi$ scattering will be made. The tree amplitude will simply be identified with K in Eq. (1.1). The interesting question about the treatment of $\pi\pi$ scattering is whether it can fit the experimental data, given the complicated strong interferences between the σ, σ' and contact term contributions. The interesting question about the πK scattering concerns the properties of the κ meson in the present model. Finally the $\pi\eta$ scattering is of methodological interest. This is because the well-established $a_0(980)$ resonance is expected to appear in a very clean way, lacking interference from a strong contact term (or even the possibility of potential interference when vector mesons are added to the model), as explained, for example in [24].

We will first carry out the calculations using the standard renormalizable form of the three flavor linear sigma model. This is characterized by the potential in Eq. (1.21). Then the whole model is extremely predictive. After using as input the well-established masses of the pseudoscalar nonet and pion decay constant [Eq. (1.14)] there is only one quantity left to choose in order to specify the scattering amplitudes. This one quantity may be taken to be the bare σ mass, $m_{\mathrm{BARE}}(\sigma)$. The corresponding values of $m_{\mathrm{BARE}}(\sigma')$ and θ_s are given in Fig. 1. We shall also carry out the calculations for the most general chiral symmetric potential. This allows $m_{\mathrm{BARE}}(\sigma')$ and θ_s to be freely chosen, which is helpful for fitting experiment. As a possible justification for using a non-renormalizable potential we mention that the model is an effective one rather than the underlying QCD. (It may be considered, for example, to be a Wilson-type effective low energy Lagrangian. While non-renormalizable terms in the potential are technically irrelevant they play a part in establishing the spontaneously broken vacuum state and should be retained.) In any event the extra parameters are being added in a chiral symmetric way.

A. $\pi\pi$ scattering

The elastic amplitude for the three flavor linear sigma model in the tree approximation was given in Eq. (1.18) above. Calculating the I=J=0 partial wave amplitude as in Sec. II A gives a result which is a straightforward generalization of Eq. (2.8):

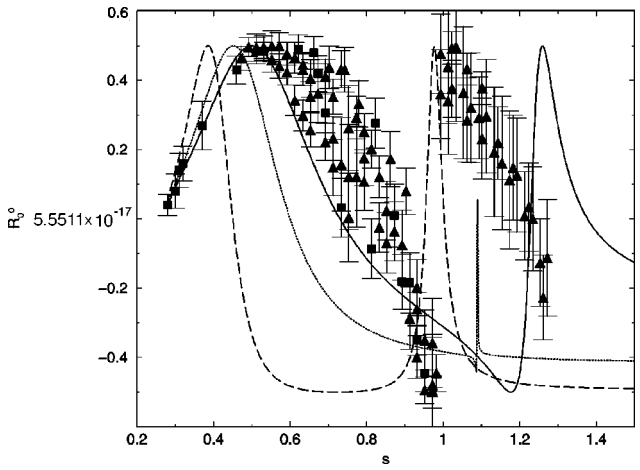

FIG. 7. Comparison with experiment of real part of the I=J=0 $\pi\pi$ scattering amplitude in the renormalizable SU(3) linear sigma model, for $m_{\mathrm{BARE}}(\sigma)=0.45$ GeV (dashes), $m_{\mathrm{BARE}}(\sigma)=0.6$ GeV (dots) and $m_{\mathrm{BARE}}(\sigma)=0.73$ GeV (solid).

$$T^0_{0\mathrm{tree}}(s)=\cos^2\psi\left[\alpha(s)+\frac{\beta(s)}{m^2_{\mathrm{BARE}}(\sigma)-s}\right]+\sin^2\psi\left[\tilde{\alpha}(s)+\frac{\tilde{\beta}(s)}{m^2_{\mathrm{BARE}}(\sigma')-s}\right], \qquad (3.2)$$

where $\tilde{\alpha}(s)$ and $\tilde{\beta}(s)$ are respectively gotten by replacing $m_{\mathrm{BARE}}(\sigma)\to m_{\mathrm{BARE}}(\sigma')$ in $\alpha(s)$ and $\beta(s)$ of Eq. (2.9). The formula (3.2) evidently represents a sum of the σ and σ' related contributions, weighted by coefficients depending on the bare $\sigma-\sigma'$ mixing angle ψ. As before, we investigate the unitarized amplitude based on Eq. (3.2):

$$T^0_0(s)=\frac{T^0_{0\mathrm{tree}}(s)}{1-iT^0_{0\mathrm{tree}}(s)}, \qquad (3.3)$$

which is being interpreted as an approximation to including the effects of the higher order corrections.

First, consider the renormalizable model. To see how well it predicts the interesting I=J=0 amplitude we may simply plot the real part of Eq. (3.3), $R^0_0(s)$ against s for various choices of the single undetermined parameter $m_{\mathrm{BARE}}(\sigma)$. (Since we are working in an elastic, exactly unitary approximation, the imaginary part of the amplitude directly follows from the real part.) Clearly the effect of the σ' contribution is small when the mixing angle ψ is small. Then one returns to the two flavor case discussed in Sec. II. Recalling that $\psi\approx\theta_s+54.7°$ and referring to the second of Fig. 1 shows that this will be the case when $m_{\mathrm{BARE}}(\sigma)$ is around 0.6 GeV. $R^0_0(s)$ for this case is shown as the dotted line in Fig. 7. The experimentally derived points [44] are included for comparison. This looks similar to the curves for the two flavor case shown in Fig. 5, except that a sharp blip appears at about 1.09 GeV corresponding to the σ' pole in $T^0_{0\mathrm{tree}}$. Note, as can be seen from Eq. (2.14), that the real part $R^0_0(s)$ will vanish both at $\sqrt{s}=m_{\mathrm{BARE}}(\sigma)$ and $\sqrt{s}=m_{\mathrm{BARE}}(\sigma')$. We saw in Sec. II B that the strong interference with the background appreciably changes the position of the physical pole in the complex s plane so, while useful for understanding Fig. 7, these zeroes of R^0_0 do not give true parametrizations of the pole position.

We have already learned that the choice $m_{\mathrm{BARE}}(\sigma)=0.6$ GeV is too low for a good fit to $R^0_0(s)$ in the region of $\sqrt{s}$ up to about 0.6 GeV. Increasing $m_{\mathrm{BARE}}(\sigma)$ improves the fit to this region and also allows the effects of the σ' to come into play. This is shown as the solid line in Fig. 7 which corresponds to the choice $m_{\mathrm{BARE}}(\sigma)=0.73$ GeV. Unfortunately (as expected from Fig. 5) this choice is still not high enough for a good fit in the low energy region. Furthermore, the structure which should correspond to the experimental $f_0(980)$ resonance has been pushed too high. Increasing $m_{\mathrm{BARE}}(\sigma)$ further will, as the first of Fig. 1 shows, push this structure even higher. One still must check to see if lowering $m_{\mathrm{BARE}}(\sigma)$ below 0.6 GeV can work. The dashed line in Fig. 7 shows $R^0_0(s)$ for $m_{\mathrm{BARE}}(\sigma)=0.45$ GeV. In this case the structure near the $f_0(980)$ is in the right place but much too narrow. The structure at lower energies is also very badly distorted.

By examining the evolution with increasing $m_{\mathrm{BARE}}(\sigma)$ of the three curves in Fig. 7, one sees that it is not possible to get a good fit for any choice of $m_{\mathrm{BARE}}(\sigma)$. Nevertheless the qualitative prediction of $R^0_0(s)$ is clearly a sensible one. It is therefore tempting to see if there is an easy way to fix up the fit.

In a sense, the difficulty in obtaining a good fit arises because only one parameter—taken to be $m_{\mathrm{BARE}}(\sigma)$—is available for adjustment to give agreement with a rather complicated experimental shape. The easiest way to proceed is to modify some parameters involved in the calculation. If a parameter to be varied is arbitrarily chosen there is however a danger of breaking the chiral symmetry relations intrinsic to the model. For example, suppose we choose to vary the coupling constant of the bare sigma to two pions. This three-point coupling constant, as mentioned in Sec. I, is related to the masses of the particles involved (see Appendix). Then, changing it without changing the masses will break the underlying chiral symmetry. Of course, we have written the formula for the tree amplitude, Eq. (1.18) in such a way that the correct relations for the 4 and 3 point coupling constants are automatically taken into account for any choice of the contained parameters $m_{\mathrm{BARE}}(\sigma)$, $m_{\mathrm{BARE}}(\sigma')$ and θ_s. In fact these three parameters may be freely chosen in the linear sigma model Eq. (1.5) with an arbitrary chiral invariant potential, V_0. It is only by restricting V_0 to be renormalizable that one can relate $m_{\mathrm{BARE}}(\sigma')$ and θ_s to $m_{\mathrm{BARE}}(\sigma)$. Thus we can freely vary $m_{\mathrm{BARE}}(\sigma')$ and θ_s in addition to $m_{\mathrm{BARE}}(\sigma)$ if we choose to obtain the tree amplitude from the nonrenormalizable model of Eq. (1.5).

In such a model it is easy to fit the experimental data for $R^0_0(s)$. A best fit obtained using the MINUIT package is shown in Fig. 8. It corresponds to the parameter choices $m_{\mathrm{BARE}}(\sigma)=0.847$ GeV, $m_{\mathrm{BARE}}(\sigma')=1.30$ GeV and $\psi=48.6°$. The physical masses and widths are obtained, as in

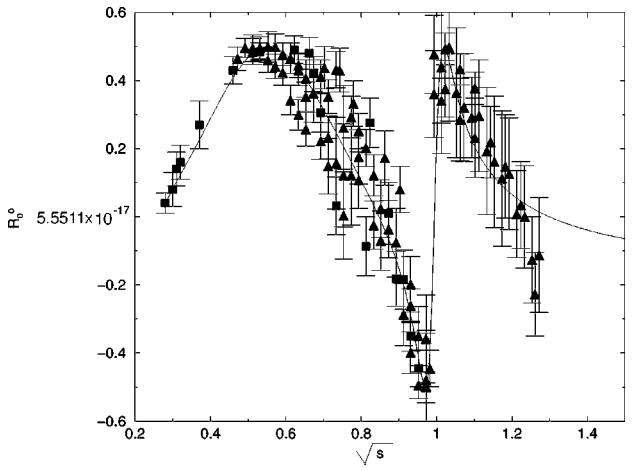

FIG. 8. Comparison of our best fit for the real part of the I=J=0 $\pi\pi$ scattering amplitude in the non-renormalizable SU(3) linear sigma model with experiment.

Eq. (2.20) in the two flavor case, from the pole positions in the complex s plane. These, together with the residues at the poles, are listed in Table II.

For orientation we first note that the parameters describing the lower mass scalar, σ are in the same range, as expected, as the parameters of Table I which give good fits to the low energy data using the σ in the two flavor case. In fact the masses are very close to each other but the effect of the additional flavor requires a somewhat greater width parameter. The contribution of the σ-pole to $T_0^0(s)$ is read off as

$$\frac{a_\sigma}{s-z_\sigma}=\frac{-a_\sigma}{m_\sigma^2-s-im_\sigma\Gamma_\sigma}=\frac{-0.167-i0.210}{0.209-s-i0.289}. \quad (3.4)$$

Note that this form is very different from a pure Breit-Wigner form which would require the numerator to be 0.289 GeV^2. This illustrates (as does the two flavor case) the importance of the interplay between the resonance and the ''background.'' It also illustrates the possible difficulty of trying to get properies of the σ from experiment with the use of a pure Breit-Wigner approximation. Note (again) from Table II that the physical mass and width, m_σ and Γ_σ respectively, are very much reduced from their bare values. The detailed mechanism is evidently similar to what we described in Sec. II for the two flavor case. It seems reasonable to consider the physical values of m_σ and Γ_σ to be the ones which are significant.

TABLE II. Physical σ and σ' parameters obtained from best fit using non-renormalizable SU(3) linear sigma model.

	σ	σ'
$m_{\rm BARE}$ (GeV)	0.847	1.300
$\Gamma_{\rm BARE}$ (GeV)	0.830	4.109
m (GeV)	0.457	0.993
Γ (GeV)	0.632	0.051
z (GeV^2)	0.209−i 0.289	0.986−i 0.051
a (GeV^2)	0.167+i 0.210	0.053−i 0.005
b	−0.248+0.856 i	

The well-established resonance $f_0(980)$ will be identified with the σ'. The contribution of the σ' pole to $T_0^0(s)$ is read off as

$$\frac{a_{\sigma'}}{s-z_{\sigma'}}=\frac{-a_{\sigma'}}{m_{\sigma'}^2-s-im_{\sigma'}\Gamma_{\sigma'}}=\frac{-0.053+i0.005}{0.986-s-i0.051}. \quad (3.5)$$

In this case the form of a pure Breit-Wigner would require that the numerator be $+0.051$ GeV^2. To a reasonable approximation this holds except for an overall sign. Now reference to the formula Eq. (2.18) for a Breit-Wigner with a background, shows that the background phase $\delta_{\rm bg}=\pi/2$ must be supplying this negative sign. Clearly the negative sign is required by the experimental data showing the real part $R_0^0(s)$ to be negative before and positive after the resonance at about 1 GeV. It was noted [12] that this is an example of the well-known Ramsauer-Townsend effect in scattering theory. It is also interesting to observe from Table II that the bare mass of the σ' is substantially shifted down from 1.300 GeV [where a zero of $R_0^0(s)$ remains, as previously discussed] to about 1 GeV. The bare width is even more substantially shifted from about 4 GeV to 50 MeV.

One might wonder whether the simple pole dominance approximation Eq. (2.21) for the two flavor case can be generalized to this more complicated three flavor case containing two poles. It turns out to be true; the prediction of our model can be numerically approximated by the sum of the two pole terms and a suitably chosen constant:

$$T_0^0(s)=R_0^0(s)+iI_0^0(s)\approx\frac{a_\sigma}{s-z_\sigma}+\frac{a_{\sigma'}}{s-z_{\sigma'}}+b, \quad (3.6)$$

where the numbers a_σ, $a_{\sigma'}$, z_σ, $z_{\sigma'}$ and b are listed in Table II. This is illustrated in Fig. 9 for $R_0^0(s)$ and $I_0^0(s)$. In these figures Eq. (3.6) is being compared with our prediction in Fig. 8. Of course, there is no reason to use Eq. (3.6) instead of the more accurate and complicated formula Eq. (3.3) but it nicely shows the dominating effect of the poles. The pole approximation is seen however not to be very accurate near threshold.

Incidentally the deep dip in $I_0^0(s)$ at what we have found to be the σ' physical pole position also represents the Ramsauer-Townsend effect. This appears in $R_0^0(s)$ as a ''flipped'' resonance curve, as discussed above. Actually this Ramsauer-Townsend phenomenon can be pictured in an alternative manner. If we consider $R_{0\rm tree}^0(s)$ corresponding to two ''bare'' resonances, one following the other, we see that there must be a point in between them where $R_{0\rm tree}^0=0$. Then Eq. (3.3) shows that, after K-matrix unitarization, R_0^0 will also vanish at this point. This point appears visually as the pole position zero of a ''flipped'' standard resonance curve. In the Ramsauer-Townsend interpretation the flipping is interpreted as a background phase of $\pi/2$. Our explicit determination of the pole positions for the sigma model amplitude

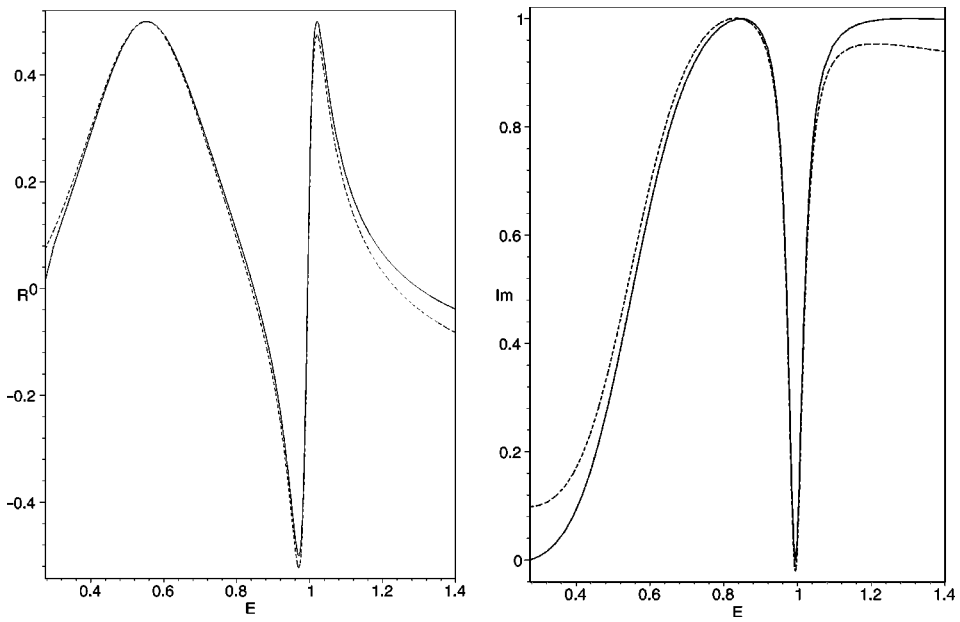

FIG. 9. Comparison of (left) real and (right) imaginary parts of pole approximation Eq. (3.6) (dashed line) with those of our predicted amplitude Eq. (3.2) (solid line).

shows that this is the pole which captures the dynamics of the $f_0(980)$. Its narrow width is seen to be the result of its getting ''squeezed'' between two nearby ''bare'' poles by the unitarization in this model.

B. πK scattering

We are interested in the I=1/2, J=0 scattering amplitude in order to investigate the properties of the κ resonance in the direct channel. The tree level amplitude involves κ exchanges in the s and u channels, σ and σ' exchanges in the t channel as well as a four point contact term. The relevant tree level invariant amplitude may be written as

$$A^{1/2}(s,t,u) = -g_K^{(4)} + \frac{3}{2}\frac{g^2_{\kappa K\pi}}{m^2_{\rm BARE}(\kappa)-s} - \frac{1}{2}\frac{g^2_{\kappa K\pi}}{m^2_{\rm BARE}(\kappa)-u} - \frac{g_{\sigma\pi\pi}g_{\sigma KK}}{m^2_{\rm BARE}(\sigma)-t} - \frac{g_{\sigma'\pi\pi}g_{\sigma' KK}}{m^2_{\rm BARE}(\sigma')-t}, \tag{3.7}$$

where s, t and u are the usual Mandelstam variables. The four point contact interaction $g_K^{(4)}$ and the bare three point coupling constants shown are listed in the Appendix. As for the cases of σ and σ' we have put a subscript BARE on the κ mass to indicate that the location of the physical pole after unitarization may come out different from this. The scalar partial wave tree amplitude is next defined by

$$T^{1/2}_{0\rm tree} = \rho(s)\int_{-1}^{1} d\cos\theta\, A^{1/2}(s,t,u). \tag{3.8}$$

Note that $\rho(s)$ was already defined by Eqs. (2.6) and (2.7). The specific formula for Eq. (3.8) in the present model is a bit lengthy and is shown in the Appendix.

According to our plan we do not introduce any new parameters for unitarization and simply write

$$T_0^{1/2} = \frac{T^{1/2}_{0\rm tree}}{1 - iT^{1/2}_{0\rm tree}}, \tag{3.9}$$

which is related to the corresponding S-matrix element by Eq. (1.1).

As mentioned in the Introduction the value of $m_{\rm BARE}(\kappa)$ is independent of whether or not the chiral invariant potential in Eq. (1.5) is renormalizable, but depends only on the set of input parameters [e.g. Eq. (1.14)]. This may be seen from the equation

$$m^2_{\rm BARE}(\kappa) = \frac{F_K m_K^2 - F_\pi m_\pi^2}{F_K - F_\pi} \tag{3.10}$$

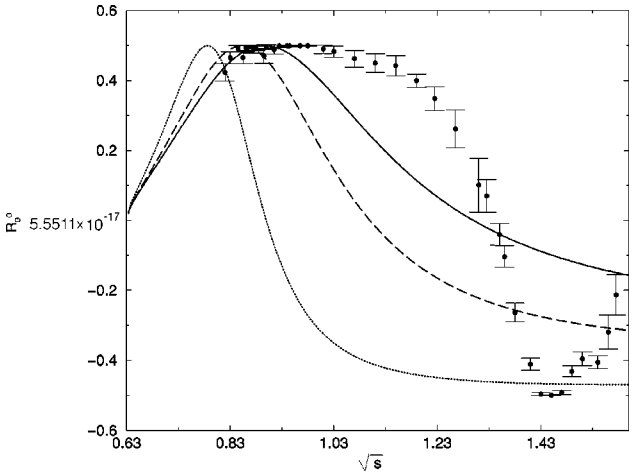

FIG. 10. Comparison of our prediction for the real part of the I=$\frac{1}{2}$, J=0 πK scattering amplitude in the non-renormalizable SU(3) linear sigma model with experiment. The curves correspond to $m_{\rm BARE}(\kappa)=1.3$ GeV (solid), 1.1 GeV (dashed) and 0.9 GeV (dotted). The experimental data are extracted from [45].

TABLE III. Physical κ parameters obtained in the non-renormalizable SU(3) linear sigma model for different values of $m_{\mathrm{BARE}}(\kappa)$ which result from different choices of input parameters.

$m_{\mathrm{BARE}}(\kappa)$ (GeV)	0.9	1.1	1.3
$\frac{F_K}{F_\pi}$, θ_p	1.4, 2.5°	1.23, −4.6°	1.16, −8.8°
$\Gamma_{\mathrm{BARE}}(\kappa)$ (GeV)	0.403	1.138	2.35
m_κ (GeV)	0.799	0.818	0.798
Γ_κ (GeV)	0.257	0.461	0.614
z_κ (GeV^2)	0.639−i 0.205	0.669−i 0.378	0.637−i 0.490
a_κ (GeV^2)	−0.043+i 0.190	0.096+i 0.340	0.263+i 0.378
b_κ	−0.438+i 0.420	−0.419+i 0.660	−0.357+i 0.800

which follows from Eqs. (1.9), (1.12) and (1.17) in the isotopic spin invariant limit. This means that there are no new unknown quantities beyond those used in the fit to the $\pi\pi$ scattering amplitude above. However we observe that the predicted value of $m_{\mathrm{BARE}}(\kappa)$ is very sensitive to the difference $F_K - F_\pi$. Actually the choice of input parameters given in Eq. (1.14) results in a somewhat too high prediction for F_K, as mentioned before.

One might therefore wonder whether the choice of input parameters in Eq. (1.14) unfairly biases our treatment of πK scattering by giving a too small value for $m_{\mathrm{BARE}}(\kappa)$. In order to check this we will also consider the slightly different choice of input parameters[8] $(m_\pi, m_K, m_{\eta'}, F_\pi, F_K)$. This will not affect the $\pi\pi$ scattering results in the non-renormalizable model just discussed. We first choose $F_K = 1.16 F_\pi$ which is slightly smaller than the physical value but has the advantage that it gives $m_{\mathrm{BARE}}(\kappa) = 1.3$ GeV which yields a zero for $T_0^{1/2}(s)$ at 1.3 GeV, in agreement with the experimental data. For this new input set we also have explicitly checked that there is still no possibility of getting a good fit to $\pi\pi$ scattering in the renormalizable model.

With this choice of input and other coupling constants taken in agreement with those found in the best fit to $\pi\pi$ scattering we have the prediction for the real part of the amplitude $R_0^{1/2}(s)$ shown in Fig. 10. The experimental data [45], which start around 0.83 GeV and go to about 1.6 GeV are also shown in this graph. It is seen that the prediction from the linear sigma model agrees with the data from about 0.83 GeV to about 0.92 GeV. However at higher energies the predicted curve lies much too low until about 1.35 GeV and thereafter seems to completely miss the structure which is usually associated with the $K_0^*(1430)$ resonance.

Figure 10 also shows the predictions for the cases when $m_{\mathrm{BARE}}(\kappa) = 1.1$ GeV (corresponding to F_K taking its experimental value) and $m_{\mathrm{BARE}}(\kappa) = 0.9$ GeV [corresponding to the input choice of Eq. (1.14)]. These are in worse agreement with the experiment and also seem to miss the $K_0^*(1430)$ structure.

As in the two flavor $\pi\pi$ case, which also contains only a single direct channel resonance we have found that the predicted amplitude is fairly well approximated as the sum of a pole term and a constant:

$$T_0^{1/2}(s) \approx \frac{a_\kappa}{s - z_\kappa} + b_\kappa . \tag{3.11}$$

The values for z_κ, a_κ and b_κ corresponding to the three different choices of input parameters are shown in Table III. Again we identify the physical mass and width by

$$m_\kappa^2 - i m_\kappa \Gamma_\kappa = z_\kappa . \tag{3.12}$$

It is notable that the pole position mass is always close to 800 MeV regardless of the choice of $m_{\mathrm{BARE}}(\kappa)$. Furthermore the widths obtained from Eq. (3.12) are substantially reduced from their ''bare'' (tree level) values, but are more sensitive to the choice of $m_{\mathrm{BARE}}(\kappa)$.

All in all, the properties of the κ obtained here are very analogous to those of the σ in either the two or three flavor treatments of $\pi\pi$ scattering. Compare with Fig. 5, for example.

It does seem that the pole mass, Eq. (3.12), of the κ is a good indication of the energy region where it provides a reasonable fit to the data. It also seems clear that the physics associated with the higher mass $K_0^*(1430)$ is not being taken into account in this model.

C. $\pi\eta$ scattering

The tree level invariant amplitude takes the form

$$A^1(s,t,u) = -g_\eta^{(4)} + g_{a_0\pi\eta}^2 \left[\frac{1}{m_{\mathrm{BARE}}^2(a_0) - s} + \frac{1}{m_{\mathrm{BARE}}^2(a_0) - u} \right] + \frac{g_{\sigma\pi\pi} g_{\sigma\eta\eta}}{m_{\mathrm{BARE}}^2(\sigma) - t} + \frac{g_{\sigma'\pi\pi} g_{\sigma'\eta\eta}}{m_{\mathrm{BARE}}^2(\sigma') - t}, \tag{3.13}$$

where the four point contact term $-g_\eta^{(4)}$ as well as the three point coupling constants are listed in the Appendix. Other conventions are the same as above. Similarly the scalar partial wave amplitude is

[8]We then predict $m_\eta \approx 0.53$ GeV rather than the experimental value of 0.547 GeV.

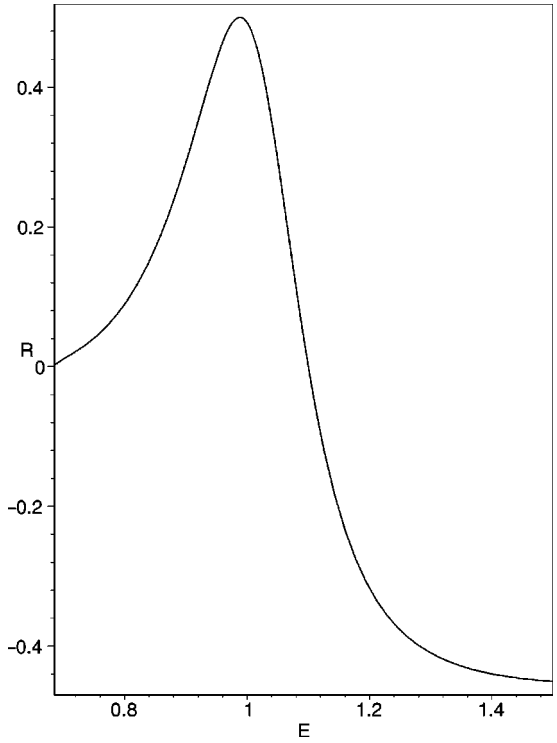

FIG. 11. Prediction for the real part of the I=1, J=0 $\pi\eta$ partial wave scattering amplitude Eq. (3.15) in the non-renormalizable SU(3) linear sigma model (parameters as in second column of Table IV).

$$T^1_{0tree}=\rho(s)\int_{-1}^{1} d\cos\theta A^1(s,t,u), \tag{3.14}$$

which is also listed in the Appendix. Again we unitarize by substituting this into the formula

$$T^1_0=\frac{T^1_{0tree}}{1-iT^1_{0tree}}. \tag{3.15}$$

Since there is apparently no experimental phase shift analysis available for this channel, we will have to be content to just present our theoretical results and compare with the mass and width of the experimental $a_0(980)$ resonance. It was already noted that the renormalizable model [with the inputs Eq. (1.14)] yields the somewhat too low bare mass (which gets shifted down by unitarization) of 913 MeV. We will also present the results for the non-renormalizable model which gave a good picture of $\pi\pi$ scattering and for which we are still free to choose $m_{\rm BARE}(a_0)$. A value $m_{\rm BARE}(a_0)=1.100$ GeV gives roughly the correct ''physical mass'' and the plot of the real part of Eq. (3.15) for this choice is shown in Fig. 11. The result of the regularization is generally similar to the curves obtained for the σ in $\pi\pi$ scattering and the κ in πK scattering. We have found in this case too that the predicted amplitude is reasonably well approximated by the sum of a pole and a constant:

TABLE IV. Physical a_0 parameters in renormalizable (first column) and non-renormalizable (second column) SU(3) linear sigma model using corresponding best-fit parameters from $\pi\pi$ scattering.

$m_{\rm BARE}(a_0)$ (GeV)	0.913	1.100
$\Gamma_{\rm BARE}(a_0)$ (GeV)	0.129	0.381
m_{a_0} (GeV)	0.890	1.013
Γ_{a_0} (GeV)	0.109	0.241
z_{a_0} (GeV^2)	0.793−i 0.097	1.027−i 0.244
a_{a_0} (GeV^2)	−0.065+i 0.064	−0.076+i 0.200
b_{a_0}	−0.299+i 0.204	−0.312+i 0.408

$$T^1_0(s)=\frac{a_{a_0}}{s-z_{a_0}}+b_{a_0}. \tag{3.16}$$

The physical mass and width are found from

$$m^2_{a_0}-im_{a_0}\Gamma_{a_0}=z_{a_0} \tag{3.17}$$

and the appropriate values for the two cases mentioned are listed in Table IV. While Fig. 11 seems to be just what one would expect for the real part of a resonance amplitude, Table IV, as in the previous cases, reveals some interesting features. First, since a_{a_0} is clearly different from $-\mathrm{Im}(z_{a_0})$, the resonance is not a pure Breit-Wigner resonance. The location of the physical pole is close to the positive peak of $R^1_0(s)$ rather than to its zero, as would hold for a Breit-Wigner resonance. Compared to the scalar resonance $\pi\pi$ and πK channels we notice that there are smaller shifts going from $m_{\rm BARE}(a_0)$ to m_{a_0} and from $\Gamma_{\rm BARE}(a_0)$ to Γ_{a_0}. This is reasonably interpreted as due to less effect of interference with the background. This is manifest in the non-linear sigma model approach to $\pi\eta$ scattering [24] and can thus be understood as a consequence of the similarity of the non-linear and linear chiral models. In addition, we note that Γ_{a_0} is predicted to be somewhat larger than the experimental value [46] of 50–100 MeV. Nevertheless, the prediction is qualitatively reasonable.

IV. SUMMARY AND DISCUSSION

We have treated the three flavor linear sigma model as a ''toy model'' for examining the role of possible light scalar mesons in the $\pi\pi$, πK and $\pi\eta$ scattering channels. This is a highly predictive model which contains only one free parameter, which may be taken as $m_{\rm BARE}(\sigma)$, in the renormalizable case. If we give up renormalizability for this effective Lagrangian but maintain chiral symmetry in a straightforward way, $m_{\rm BARE}(\sigma')$, the scalar mixing angle θ_s and $m_{\rm BARE}(a_0)$ may also be freely chosen, which is helpful for fitting experiment in the desired energy range of threshold to the 1+ GeV region. Our approach just involves computing the tree amplitude for each channel and unitarizing by a simple ''K-matrix'' prescription which does not itself introduce any new parameters. In general the unitarization has very important effects converting ''bare'' scalar meson masses and widths into ''physical'' ones. It turns out that

TABLE V. Predicted ''physical'' masses and widths in MeV of the nonet of scalar mesons contrasted with suitable (as discussed in the text) comparison values.

	σ	f_0	κ	a_0
Present Model				
mass (MeV), width (MeV)	457, 632	993, 51	800, 260–610	890–1010, 110–240
Comparison				
mass (MeV), width (MeV)	560, 370	980 ± 10, 40–100	900, 275	985, 50–100

there is not too much ''wiggle room'' in this procedure so that what results is characteristic of the model (and the unitarization scheme). This tightness comes from the demand that the starting tree amplitudes satisfy chiral symmetry restrictions. This means, as discussed in Sec. I, that the four point contact interaction vertices are related to the three point interactions which are related to the particle masses (two point objects) which are related in turn to the one point terms (pseudoscalar meson decay constants). We chose the inputs to be the four pseudoscalar masses and the pion decay constant [Eq. (1.14)]. However the pseudoscalar mixing angle and kaon decay constant were not perfectly predicted so there is already a source of error present before even going to the scattering amplitudes. Nevertheless we investigated this point by considering an alternative input set obtained by using F_K instead of m_η and found that there was not much qualitative change for the scattering predictions.

Our point of view in this paper is to see what are the results of computing in a relatively simple and natural model for the purpose of comparison with other (and possibly future) more elaborate treatments. It seems to us that the results are interesting and instructive. In the simpler two flavor case, which was applied in [4] to a lower energy treatment of $\pi\pi$ scattering, the results were already reasonable. Here we have, in Sec. II, reviewed the two flavor case in a slightly different way as preparation for the more complicated three flavor case. We have also made some new comments and suggested an alternative ''naive'' unitarization procedure which might be handy for future studies.

Table V contains a brief summary of the physical masses and widths of the scalar mesons predicted in the present model and discussed in some detail in Sec. III. In the cases of the $f_0(980)$ and $a_0(980)$ resonances comparison is being made with experimental values [46]. In the cases of the σ and the κ, which are less well-established experimentally, we have compared with the earlier computations of the Syracuse group [12,14,15] which were based on a non-linear chiral effective Lagrangian treatment, including vector mesons. Many other authors [30] were led to similar predictions for the σ while similar predictions for the κ were made in [11] and the third of [16]. Answers to the concerns expressed in [47] on the experimental existence of the κ were made in [14], the third of [16] and in [48].

The predicted properties of the σ and f_0 in the present model come from their role in $\pi\pi$ scattering as discussed in Sec. III A. It was found that the single parameter describing the renormalizable model could not be adjusted to give a reasonable fit to the experimental data. This could be done when the renormalizability condition was relaxed. Neither the physical σ nor the physical f_0 are described by simple Breit-Wigner terms. Both have masses and widths greatly reduced from their ''bare'' values by the unitarization procedure. The light, broad σ is somewhat lighter and broader than the comparison one obtained in the non-linear model [12]. (However when the vector meson contribution in the non-linear model was consistently eliminated [13] the σ in that model also became broader and lighter.) The f_0 obtained approximately looked like a Breit-Wigner in a background which has a phase $\delta_{bg} = \pi/2$. This is known as the Ramsauer-Townsend effect in scattering theory. The fact that it emerges in the present model was noted to be explicable in terms of the region between two neighboring ''bare'' resonances getting squeezed by unitarization.

The entries in Table V for the κ mass and width require some explanation. The bare κ mass and width in this model are uniquely predicted once the input parameters are specified, regardless of whether or not the potential is taken to be renormalizable. However the predictions of the κ parameters are very sensitive to F_K [which measures the deviation of the vacuum from exact SU(3) flavor symmetry in this model]. Thus we allowed different input sets yielding different bare κ masses, as discussed in Sec. III B. Whatever reasonable choice was made, the unitarization always brought the physical κ mass down to around 800 MeV. However the physical width is more dependent on this choice. Furthermore, as shown in Fig. 10, the κ resonance can only explain the lower energy πK scattering data. This would be the analog of the SU(2) treatment of $\pi\pi$ scattering, where the σ alone can provide a reasonable description of the low energy region. The κ cannot explain the data in the region of the $K_0^*(1430)$ scalar resonance. In other words, we cannot explain the $K_0^*(1430)$ as the strange scalar of the usual linear sigma model treated with K-matrix unitarization.

In the case of the $\pi\eta$ channel there does not appear to be any experimental phase shift data, so we compare with experimental determinations of the $a_0(980)$ mass and width. The lower physical mass entry for the a_0 in Table V corresponds to the bare mass of the renormalizable model. It is somewhat too low but not very far off. This can be easily adjusted by using the non-renormalizable potential. The predicted width is somewhat too large but qualitatively reasonable. Clearly, the a_0 of the present model is describing the low energy part of $\pi\eta$ scattering and should correspond to the $a_0(980)$ rather than the $a_0(1450)$.

All in all, the three flavor linear sigma model with a general (non-renormalizable) chiral invariant potential and regularized by the simple K-matrix procedure can approximately

describe the complicated $\pi\pi$ scalar scattering amplitude as well as the low energy part of the $K\pi$ scalar amplitude and the $a_0(980)$ $\pi\eta$ resonance. The $K_0^*(1430)$ and $a_0(1450)$ are ''outsiders'' in this picture and would have to be put in by hand to realize the higher mass scalar resonances in πK and $\pi\eta$ scattering. The picture is qualitatively similar to that obtained in treatments using the non-linear sigma model for $\pi\pi$ [12], πK [14] and $\pi\eta$ [24] scattering. The $a_0(980)$ and $f_0(980)$ seem to belong to the same multiplet as the controversial light σ and light κ. Of course, it is possible for particles with the same quantum numbers belonging to other multiplets to mix with them.

There are several straightforward, but lengthy to carefully implement, ways to improve this treatment. Modified kinetic terms, as mentioned in Sec. I, can be included to improve the fit to pseudoscalar masses and decay constants. Vector and axial vector mesons can be added to introduce more of the low-lying physical resonances which are expected to be important in the $\pi\pi$ and πK channels. Certainly, inelastic channels should be included. In the treatment of $\pi\pi$ scattering using the non-linear model in [12] it was found that taking some account of the $K\bar{K}$ channel did not change the basic structure of the elastic scattering amplitude for the energy range considered here. Since the unitarization procedure played an important role in our analysis it seems very desirable to investigate more ''dynamical'' methods than the conventional *K*-matrix scheme employed here. A promising scheme which introduces one new parameter has been recently suggested by Oller and Meissner [49].

V. SPECULATION ON SCALAR MESON'S QUARK STRUCTURE

Up to this point we have reported the results of a straightforward and highly predictive treatment of the three flavor linear sigma model. Our original reason for pursuing this investigation was to check the results obtained in our treatment of meson scattering in the non-linear sigma model which contained additional particles and channels. That treatment used a different unitarization procedure in which crossing symmetry and unitarity were both approximately satisfied. (Actually in the study of direct channel scalar resonances, the crossed scalar exchanges are relatively small.) We already noted that the locations and widths of the *physical* scalar states obtained in the linear model were qualitatively similar to those obtained in the non-linear model. Since the σ, f_0, a_0 and κ all come out less than or about 1 GeV, and the scattering regions near the $a_0(1450)$ and the $K_0^*(1430)$ apparently must be described by fields other than those contained in the matrix *M*, the well known puzzle of the quark structure of these scalars comes to the surface.

In this section we will make some speculative remarks on this controversial subject and introduce another toy model which may illuminate some of the issues. The puzzle, of course, is why, if the scalars are ''$q\bar{q}$ states,'' they are considerably lighter than the other p-wave states and why the isovector $a_0(980)$ is tied for being the heaviest, rather than the lightest, member of the multiplet.

Actually there is a lot of ambiguity in stating what the quark structure of a physical hadron means. Generally people think of the question in the context of a potential-type model wherein, for example, the ρ meson is made of a ''constituent'' quark of mass about 300 MeV and a constituent antiquark of the same mass. The idea is that the fundamental ''current quarks of QCD'' (with masses about 10 MeV) interact strongly with each other and with gluons to make the relatively weakly interacting constituents whose combined masses roughly approximate the physical hadron masses. Thus the quark structure really depends on the model used to treat the hadrons. At the field theory level of ''current quarks'' there is always some probability for extra $q\bar{q}$ pairs or other structures to be present. In the $SU(3)_L\times SU(3)_R$ chiral effective Lagrangian treatments, the quark substructure of the fields being used does not enter the formulation in a unique way. An infinite number of different quark substructures will give rise to the same $SU(3)_L\times SU(3)_R$ transformation properties for the mesons. This is apparent for the non-linear chiral model in which scalars are added to the pseudoscalar meson Lagrangian as ''matter fields'' in the usual manner [43]. Then it is known that only the SU(3) flavor transformation properties of the scalars are relevant. However we found in our earlier study [15] that the value of the scalar mixing angle suggested indirectly that the light scalars do have an important four quark component. Considering the properties of the heavier scalars $a_0(1450)$ and $K_0^*(1430)$ suggested [25] that these states did not belong to a ''pure'' $q\bar{q}$ multiplet but to one which mixed with the lighter scalar multiplet.

When it comes to the linear sigma model where the chiral transformations of the scalars are linked with those of the pseudoscalars in a natural way, there seems to be a feeling that the matrix *M* should describe a $q\bar{q}$ field. In fact, there are still an infinite number of quark substructures which transform in the same manner under $SU(3)_L\times SU(3)_R$. It may be worthwhile to illustrate this for the specific cases of interest in the literature.

The schematic structure for the matrix $M(x)$ realizing a $q\bar{q}$ composite in terms of quark fields $q_{aA}(x)$ can be written

$$M_a^{(1)b}=(q_{bA})^\dagger\gamma_4\frac{1+\gamma_5}{2}q_{aA}, \tag{5.1}$$

where *a* and *A* are respectively flavor and color indices. Our convention for matrix notation is $M_a^{(1)b}\to M_{ab}^{(1)}$. Then $M^{(1)}$ transforms under chiral $SU(3)_L\times SU(3)_R$ as

$$M^{(1)}\to U_L M^{(1)}U_R^\dagger \tag{5.2}$$

where U_L and U_R are unitary, unimodular matrices associated with the transformations on the left handed $[q_L=\frac{1}{2}(1+\gamma_5)q]$ and right handed $[q_R=\frac{1}{2}(1-\gamma_5)q]$ quark projections. For the discrete transformations charge conjugation *C* and parity *P* one verifies

$$C:\quad M^{(1)}\to M^{(1)T},\quad P:\quad M^{(1)}(\mathbf{x})\to M^{(1)\dagger}(-\mathbf{x}). \tag{5.3}$$

Finally, the $U(1)_A$ transformation acts as $q_{aL}\to e^{i\nu}q_{aL}$, $q_{aR}\to e^{-i\nu}q_{aR}$ and results in

$$M^{(1)}\to e^{2i\nu}M^{(1)}. \tag{5.4}$$

One interesting model [50] for explaining the scalar meson puzzle [at least insofar as the $a_0(980)$ and $f_0(980)$ states are concerned] is to postulate that the light scalars are ''molecules'' made out of two pseudoscalar mesons. The chiral realization of this picture would result in the following schematic structure:

$$M_a^{(2)b}=\epsilon_{acd}\epsilon^{bef}(M^{(1)\dagger})_e^c(M^{(1)\dagger})_f^d. \tag{5.5}$$

One can verify that $M^{(2)}$ transforms exactly in the same way as $M^{(1)}$ under $SU(3)_L\times SU(3)_R$, C and P. Under $U(1)_A$ it transforms as

$$M^{(2)}\to e^{-4i\nu}M^{(2)}, \tag{5.6}$$

which differs from Eq. (5.4).

Another interesting approach [51] to explaining the light scalar mesons was formulated by Jaffe in the framework of the MIT bag model. It was observed that the spin-spin (hyperfine) piece of the one gluon exchange interaction between quarks gives an exceptionally strong binding to an s-wave $qq\overline{qq}$ scalar state. Furthermore, this model naturally predicts an ''inverted'' mass spectrum of the type summarized in Table V. A more detailed recent discussion is given in [15]. The scalar states of this type may be formally written as bound states of a ''dual quark'' and ''dual antiquark.'' There are two possibilities if the dual antiquark is required to belong to a $\overline{3}$ representation of flavor SU(3). In the first case it belongs to a $\overline{3}$ of color and is a spin singlet. This has the schematic chiral realization,

$$L^{gE}=\epsilon^{gab}\epsilon^{EAB}q_{aA}^T C^{-1}\frac{1+\gamma_5}{2}q_{bB},$$

$$R^{gE}=\epsilon^{gab}\epsilon^{EAB}q_{aA}^T C^{-1}\frac{1-\gamma_5}{2}q_{bB}, \tag{5.7}$$

where C is the charge conjugation matrix of the Dirac theory. A suitable form for the M matrix is

$$M_g^{(3)f}=(L^{gA})^\dagger R^{fA}. \tag{5.8}$$

$M^{(3)}$ can be seen to transform in the same way as $M^{(2)}$ under $SU(3)_L\times SU(3)_R$, C, P and $U(1)_A$. In the second case the dual antiquark belongs to a 6 representation of color and has spin 1. It has the corresponding schematic chiral realization:

$$L^g_{\mu\nu,AB}=L^g_{\mu\nu,BA}=\epsilon^{gab}q_{aA}^T C^{-1}\sigma_{\mu\nu}\frac{1+\gamma_5}{2}q_{bB},$$

$$R^g_{\mu\nu,AB}=R^g_{\mu\nu,BA}=\epsilon^{gab}q_{aA}^T C^{-1}\sigma_{\mu\nu}\frac{1-\gamma_5}{2}q_{bB}, \tag{5.9}$$

where $\sigma_{\mu\nu}=(1/2i)[\gamma_\mu,\gamma_\nu]$. This choice leads to an M matrix

$$M_g^{(4)f}=(L^g_{\mu\nu,AB})^\dagger R^f_{\mu\nu,AB}, \tag{5.10}$$

where the dagger operation includes a factor $(-1)^{\delta_{\mu4}+\delta_{\nu4}}$. $M^{(4)}$ also transforms like $M^{(2)}$ and $M^{(3)}$ under all of $SU(3)_L\times SU(3)_R$, C, P and $U(1)_A$. The specific form favored by the MIT bag model calculation actually corresponds to a particular linear combination of $M^{(3)}$ and $M^{(4)}$. Furthermore one can verify that $M^{(2)}$ in Eq. (5.5) is related by a Fierz transformation to a linear combination of $M^{(3)}$ and $M^{(4)}$. Thus only two of $M^{(2)}$, $M^{(3)}$ and $M^{(4)}$ are linearly independent. At the effective Lagrangian level the distinction between meson-meson and diquark-antidiquark models is clearly blurred.

What is the significance of these remarks for construction of the general effective chiral Lagrangian used in this paper [Eq. (1.5)]? All that is required for M is that it transform like $M^{(1)}$ under $SU(3)_L\times SU(3)_R$, C and P and that it carry a non-zero $U(1)_A$ ''charge'' which gets broken by the potential. The specific $U(1)_A$ transformation property does differ between the two quark realization $M^{(1)}$ and the four quark realizations ($M^{(2)}$, $M^{(3)}$ and $M^{(4)}$) but this would just be absorbed, in the present work, by a different value for the parameter V_4. Thus, if one knew nothing else about hadronic physics than the present toy Lagrangian, one would not be able to *a priori* easily discriminate among the possibilities $M^{(1)}-M^{(4)}$, or in fact any others, for the underlying quark substructure of the scalars (and pseudoscalars). Nevertheless, one might glance at the obtained scalar masses in Table V and notice that there is an inverted physical mass spectrum. One might then decide to make a judgement on the *constituent* quark substructure by fitting the scalar spectrum to an Okubo type mass formula [52]. This was done recently, for example, in Sec. II of [15] and suggests that the scalars are behaving roughly as composites of four constituent quarks. Roughly, this amounts to simply counting the number of strange constituent pieces in each state; in the four quark picture both $f_0(980)$ and $a_0(980)$ have two. The combined effects of spontaneous chiral symmetry breaking and unitarization (presumably taking radiative corrections into account) appears to split the constituent structures of the scalars from the pseudoscalars, regardless of which current quark structure (i.e. choice of M) we start with.

However the true situation is likely to be more complicated. The present model does not appear to accommodate the $a_0(1450)$ and $K_0^*(1430)$ scalars as states belonging to M. These states would seem at first sight to be reasonable candidates for a nonet of ordinary $q\overline{q}$ scalars. Still it is a little puzzling that $K_0^*(1430)$ is not heavier than $a_0(1450)$. There are some other puzzles too but all can be qualitatively explained [25] if a $q\overline{q}$ scalar nonet mixes with a $qq\overline{qq}$ scalar nonet. If we want to realize such a scheme in the linear model framework it would be natural to introduce a Lagrangian with two different M matrices. Such a model seems to yield a variety of interesting dynamical possibilities which may lead to new insights and approximation schemes for low energy QCD. Thus it may be worthwhile to give a brief discussion here.

Let us start with the field $M^{(1)}$ which we shall simply

designate M. At the kinematical level it represents a current-type quark antiquark operator. This is modified for both the pseudoscalar and scalar states by the (almost) spontaneous breakdown of chiral symmetry. For the scalars (which occur as poles in the physical region) there is an additional modification due to the unitarization required. Of course, the choice of the free parameters gives an ''experimental'' input to this process. The resulting scalars seem to be roughly consistent with a $\overline{qqqq}$ constituent-quark structure, as just discussed. Now consider adding a current type four quark operator which may be any combination of $M^{(2)}$, $M^{(3)}$ or $M^{(4)}$ (we could not tell the difference in an effective Lagrangian framework) and denote it by M'. Allow M' to mix with M. What happens?

The Lagrangian which directly generalizes Eq. (1.5) is written as

$$\mathcal{L}=-\frac{1}{2}\mathrm{Tr}(\partial_\mu M\partial_\mu M^\dagger)-\frac{1}{2}\mathrm{Tr}(\partial_\mu M'\partial_\mu M'^\dagger) - V_0(M,M')-V_{SB}, \tag{5.11}$$

where $V_0(M,M')$ stands for a general polynomial made from $SU(3)_L\times SU(3)_R$ [but not $U(1)_A$] invariants formed out of M and M'. Furthermore V_{SB} is taken to be the same as Eq. (1.7) since it is $\mathrm{Tr}(M+M^\dagger)$ which ''mocks up'' the quark mass terms. Other physical particles (including glueballs) could be added for more realism, but Eq. (5.11) is already quite complicated.

To get an indication of what kinds of questions might be answered, let us consider a very simplified approximation in which the quark mass effective term, V_{SB} is absent and where V_0 is simply given by

$$V_0=-c_2\mathrm{Tr}(MM^\dagger)+c_4\mathrm{Tr}(MM^\dagger MM^\dagger) + d_2\mathrm{Tr}(M'M'^\dagger)+e\,\mathrm{Tr}(MM'^\dagger+M'M^\dagger). \tag{5.12}$$

Here c_2, c_4 and d_2 are positive real constants. The M matrix field is chosen to have a wrong sign mass term so that there will be spontaneous breakdown of chiral symmetry. A pseudoscalar octet will thus be massless. On the other hand, the matrix field M' is being set up to have trivial dynamics except for its mixing term with M. The mixing is controlled by the parameter e and the e-term is the only one which violates $U(1)_A$ symmetry. Its origin is presumably due to instanton effects at the fundamental QCD level. [Other $U(1)_A$-violating terms which contribute to η' mass etc. are not being included for simplicity.] Using the notations $M=S+i\phi$ and $M'=S'+i\phi'$ we may expect vacuum values

$$\langle S_a^b\rangle=\alpha\delta_a^b,\quad \langle S_a'^b\rangle=\beta\delta_a^b. \tag{5.13}$$

The minimization condition $\langle\partial V_0/\partial S_a'^b\rangle=0$ leads to

$$\beta=-\frac{e}{d_2}\alpha \tag{5.14}$$

while $\langle\partial V_0/\partial S_a^b\rangle=0$ yields

$$\alpha^2=\frac{1}{2c_4}\left(c_2+\frac{e^2}{d_2}\right). \tag{5.15}$$

In the absence of mixing the ''four-quark'' condensate β vanishes while the usual two quark condensate α remains.

The mass spectrum resulting from Eq. (5.12) has two scalar octets and two pseudoscalar octets, each with an associated $SU(3)$ singlet. Each octet has eight degenerate members since the quark mass terms have been turned off. Let us focus on the I=1, positively charged particles for definiteness and define

$$\pi^+=\phi_1^2,\quad \pi'^+=\phi_1'^2,\quad a^+=S_1^2,\quad a'^+=S_1'^2. \tag{5.16}$$

Then the 2×2 squared mass matrix of π and π' is

$$2\begin{bmatrix}\dfrac{e^2}{d_2} & e\\ e & d_2\end{bmatrix}. \tag{5.17}$$

This has eigenstates

$$\pi_p=\left(1+\frac{e^2}{d_2^2}\right)^{-1/2}\left(\pi-\frac{e}{d_2}\pi'\right),$$
$$\pi_p'=\left(1+\frac{e^2}{d_2^2}\right)^{-1/2}\left(\frac{e}{d_2}\pi+\pi'\right), \tag{5.18}$$

with masses

$$m^2(\pi_p)=0,\quad m^2_{\mathrm{BARE}}(\pi_p')=\frac{2e^2}{d_2}+2d_2. \tag{5.19}$$

We put the subscript ''BARE'' on $m^2(\pi_p')$ to indicate that it may receive non-negligible corrections from K-matrix unitarization as in our detailed treatment of the M only Lagrangian in the above. A possible experimental candidate for such a particle is the $\pi(1300)$.

Computing the axial vector current by Noether's theorem yields

$$(J_\mu^{\mathrm{axial}})_1^2=F_\pi\partial_\mu\pi_p^+ +\cdots,$$
$$F_\pi=2\alpha\sqrt{1+\left(\frac{e}{d_2}\right)^2}, \tag{5.20}$$

where α is given in Eq. (5.15).

Notice that a term like $\partial_\mu\pi_p'^+$ does not appear in our semi-classical approximation.

The 2×2 squared mass matrix of the scalars a and a' is

$$\begin{bmatrix}4c_2+\dfrac{6e^2}{d_2} & 2e\\ 2e & 2d_2\end{bmatrix}. \tag{5.21}$$

The eigenstates are defined by

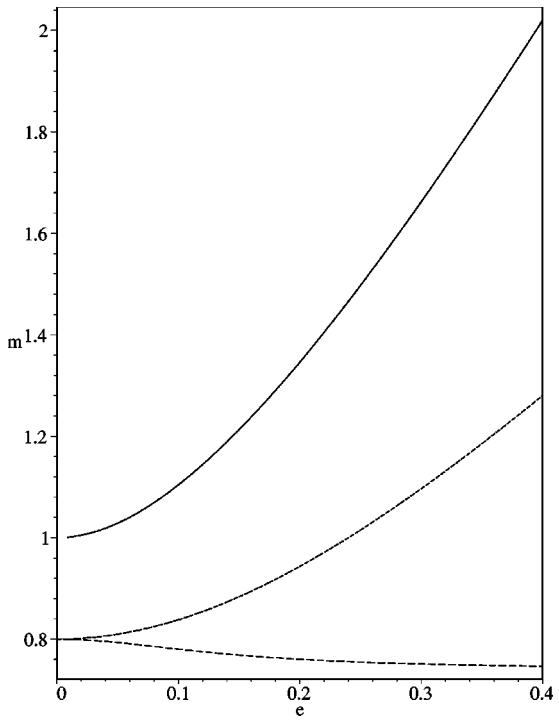

FIG. 12. Plots of $m_{\rm BARE}(a_p)$ (solid), $m_{\rm BARE}(a_p')$ (dashed) and $m_{\rm BARE}(\pi_p')$ versus the mixing parameter e for the choice $c_2=0.25$ GeV^2 and $d_2=0.32$ GeV^2. The highest lying curve is mainly a ''$q\overline{q}$'' scalar, while the lowest lying curve is mainly a ''$qq\overline{qq}$'' scalar. The excited pseudoscalar curve is in the middle.

$$\begin{pmatrix} a_p \\ a_p' \end{pmatrix} = \begin{bmatrix} \cos\omega & -\sin\omega \\ \sin\omega & \cos\omega \end{bmatrix} \begin{pmatrix} a \\ a' \end{pmatrix}, \tag{5.22}$$

with

$$\tan 2\omega = \frac{4e}{2d_2 - 4c_2 - \dfrac{6e^2}{d_2}}. \tag{5.23}$$

The corresponding masses are

$$m^2_{\rm BARE}(a_p, a_p') = 2c_2 + d_2 + \frac{3e^2}{d_2} \mp 2e \csc 2\omega, \tag{5.24}$$

where the upper (lower) sign stands for a_p, (a_p').

It is interesting to examine the masses of the degenerate octets in a little more detail. For orientation, first consider the case when the mixing parameter e vanishes. The usual ''$q\overline{q}$'' pseudoscalars π_p are zero mass Goldstone bosons in this approximation. If $4c_2 > 2d_2$, a_p, the original scalar partner of π_p lies higher than the degenerate ''$qq\overline{qq}$'' scalar and pseudoscalar a_p' and π_p'. When the mixing is turned on, a four quark condensate develops and the mass ordering is

$$m_{\rm BARE}(a_p) > m_{\rm BARE}(\pi_p') > m_{\rm BARE}(a_p') > m_{\rm BARE}(\pi_p) = 0. \tag{5.25}$$

This is graphed, as a function of e, in Fig. 12 (with parameter choices $c_2=0.25$ GeV^2, $d_2=0.32$ GeV^2). In such a scenario, the $qq\overline{qq}$ scalar would be the next lightest after the $q\overline{q}$ Goldstone boson. Each particle would be a mixture of $q\overline{q}$ and $qq\overline{qq}$ to some extent. For the given parameters the mixing angle remains small however because the denominator of Eq. (5.23) is always negative and increases in magnitude as e^2 increases. Note especially, that due to the spontaneous breakdown of chiral symmetry, there is no guarantee that the lowest lying scalar is of $q\overline{q}$ type. Also note that π_p' is expected to be more massive than a_p'.

On the other hand, if the QCD dynamics underlying the effective Lagrangian is such that $2d_2 > 4c_2$ we will get a mass ordering $m_{\rm BARE}(a_p') > m_{\rm BARE}(\pi') > m_{\rm BARE}(a_p)$ in which the four quark scalar appears heaviest. However, in this case we will definitely get a large mixing as e increases since the denominator of Eq. (5.23) starts out positive when $e=0$ and will go to zero as e is increased. Thus the next-to-lowest lying a_p can be expected to have a large $qq\overline{qq}$ admixture.

All of these remarks pertain to the meson current-quark type operators in the toy model. The important effects of unitarization (i.e. $m_{\rm BARE} \to m$) are likely, as in our earlier treatment, to favor an interpretation of the low lying physical scalars as being of four constituent quark type in either case.

The main lesson from our preliminary treatment of a chiral model with mixing is perhaps that even though the M fields carry ''chiral indices'' it is not easy to assign an unambiguous quark substructure. On the other hand there is a great potentiality for learning more about non-perturbative QCD from further study of the light scalars. Such features as scalar mixing (including the possibility of mixing with glueballs for the I=0 states), four quark condensates and excited pseudoscalars may eventually get correlated with each other and with the experimental data on the scattering of light pseudoscalars.

ACKNOWLEDGMENTS

We are happy to thank Masayasu Harada and Francesco Sannino for many helpful discussions. This work has been supported in part by the U.S. DOE under contract DE-FG-02-85ER40231. One of us (S.M.) would like to thank the Egyptian Cultural Bureau for support. A.H.F. wishes to acknowledge his grant from the State of New York/UUP Professional Development Committee.

APPENDIX: COUPLING CONSTANTS AND PARTIAL WAVE AMPLITUDES

For the scattering processes under consideration we will need the four-point pseudoscalar contact interactions and the trilinear scalar-pseudoscalar-pseudoscalar interactions. In isotopic spin notation the relevant pieces of the Lagrangian are, respectively,

$$-\mathcal{L}^{(4)} = \frac{1}{16} g_\pi^{(4)} (\boldsymbol{\pi}\cdot\boldsymbol{\pi})^2 + \frac{1}{2} g_K^{(4)} \overline{K}K \boldsymbol{\pi}\cdot\boldsymbol{\pi} + \frac{1}{4} g_\eta^{(4)} \eta\eta \boldsymbol{\pi}\cdot\boldsymbol{\pi} + \cdots \tag{A1}$$

and

$$-\mathcal{L}_{S\phi\phi}=\frac{g_{\kappa K\pi}}{\sqrt{2}}(\bar{K}\boldsymbol{\tau}\cdot\boldsymbol{\pi}\boldsymbol{\kappa}+\text{H.c.})+\frac{g_{\sigma\pi\pi}}{2}\sigma\boldsymbol{\pi}\cdot\boldsymbol{\pi}+g_{\sigma KK}\sigma\bar{K}K+\frac{g_{\sigma'\pi\pi}}{2}\sigma'\boldsymbol{\pi}\cdot\boldsymbol{\pi}+g_{\sigma' KK}\sigma'\bar{K}K$$

$$+\frac{g_{a_0KK}}{\sqrt{2}}\bar{K}\boldsymbol{\tau}\cdot\mathbf{a_0}K+g_{\kappa K\eta}(\bar{\kappa}K\eta+\text{H.c.})+g_{\kappa K\eta'}(\bar{\kappa}K\eta'+\text{H.c.})+g_{a_0\pi\eta}\mathbf{a_0}\cdot\boldsymbol{\pi}\eta+g_{a_0\pi\eta'}\mathbf{a_0}\cdot\boldsymbol{\pi}\eta'$$

$$+\frac{g_{\sigma\eta\eta}}{2}\sigma\eta\eta+g_{\sigma\eta\eta'}\sigma\eta\eta'+\frac{g_{\sigma\eta'\eta'}}{2}\sigma\eta'\eta'+\frac{g_{\sigma'\eta\eta}}{2}\sigma'\eta\eta+g_{\sigma'\eta\eta'}\sigma'\eta\eta'+\frac{g_{\sigma'\eta'\eta'}}{2}\sigma'\eta'\eta'. \tag{A2}$$

The trilinear couplings which do not involve three isoscalars are predicted in terms of the masses. These are given in [37] and we present them here for completeness:

$$g_{\kappa K\pi}=\frac{1}{F_K}(m^2_{\text{BARE}}(\kappa)-m^2_\pi),\quad g_{\kappa K\eta}=\frac{1}{\sqrt{6}F_K}(\cos\theta_p+2\sqrt{2}\sin\theta_p)(m^2_\eta-m^2_{\text{BARE}}(\kappa)), \tag{A3}$$

$$g_{\kappa K\eta'}=\frac{1}{\sqrt{6}F_K}(2\sqrt{2}\cos\theta_p-\sin\theta_p)(m^2_{\text{BARE}}(\kappa)-m^2_{\eta'})\quad g_{a_0KK}=\frac{1}{F_K}(m^2_{\text{BARE}}(a_0)-m^2_K),$$

$$g_{a_0\pi\eta}=\frac{\sqrt{2}}{F_\pi}a_p(m^2_{\text{BARE}}(a_0)-m^2_\eta),\quad g_{a_0\pi\eta'}=\frac{\sqrt{2}}{F_\pi}b_p(m^2_{\text{BARE}}(a_0)-m^2_{\eta'}),$$

$$g_{\sigma\pi\pi}=\frac{\sqrt{2}}{F_\pi}a_s(m^2_{\text{BARE}}(\sigma)-m^2_\pi),\quad g_{\sigma'\pi\pi}=\frac{\sqrt{2}}{F_\pi}b_s(m^2_{\text{BARE}}(\sigma')-m^2_\pi),$$

$$g_{\sigma KK}=\frac{1}{\sqrt{6}F_K}(\cos\theta_s+2\sqrt{2}\sin\theta_s)(m^2_K-m^2_{\text{BARE}}(\sigma)),$$

$$g_{\sigma' KK}=\frac{1}{\sqrt{6}F_K}(2\sqrt{2}\cos\theta_s-\sin\theta_s)(m^2_{\text{BARE}}(\sigma')-m^2_K).$$

The trilinear coupling constants involving three isoscalars may depend on V_4. For $\pi\eta$ elastic scattering we will also need

$$g_{\sigma\eta\eta}=\frac{a_s}{\sqrt{2}}X-b_sY,\quad g_{\sigma'\eta\eta}=\frac{b_s}{\sqrt{2}}X+a_sY, \tag{A4}$$

where

$$X=\left(\frac{a_p}{\sqrt{2}}\right)^2\frac{2}{F_\pi}[2a_s^2m^2_{\text{BARE}}(\sigma)+2b_s^2m^2_{\text{BARE}}(\sigma')-m^2_\pi-a_p^2m^2_\eta-b_p^2m^2_{\eta'}-12(2F_K-F_\pi)V_4]$$

$$+b_p^2\frac{2}{2F_K-F_\pi}[-\sqrt{2}a_sb_s(m^2_{\text{BARE}}(\sigma)-m^2_{\text{BARE}}(\sigma'))-12F_\pi V_4]+\frac{48}{\sqrt{2}}a_pb_pV_4, \tag{A5}$$

$$Y=\left(\frac{a_p}{\sqrt{2}}\right)^2\frac{2}{F_\pi}[-\sqrt{2}a_sb_s(m^2_{\text{BARE}}(\sigma)-m^2_{\text{BARE}}(\sigma'))-24F_\pi V_4]$$

$$+b_p^2\frac{2}{2F_K-F_\pi}[b_s^2m^2_{\text{BARE}}(\sigma)+a_s^2m^2_{\text{BARE}}(\sigma')-b_p^2m^2_\eta-a_p^2m^2_{\eta'}]. \tag{A6}$$

In these equations we have used the convenient abbreviations

$$a_p=\frac{\cos\theta_p-\sqrt{2}\sin\theta_p}{\sqrt{3}},\quad b_p=\frac{\sqrt{2}\cos\theta_p+\sin\theta_p}{\sqrt{3}},\tag{A7}$$

with analogous expressions for $a_s=\cos\psi$ and $b_s=\sin\psi$ in terms of θ_s. The contact coupling constants are then given by

$$g_\pi^{(4)}=\frac{4}{F_\pi^2}(a_s^2 m^2_{\rm BARE}(\sigma)+b_s^2 m^2_{\rm BARE}(\sigma')-m_\pi^2),\tag{A8}$$

$$g_K^{(4)}=\frac{1}{F_\pi F_K}[m^2_{\rm BARE}(\kappa)-m_K^2-m_\pi^2+a_s^2 m^2_{\rm BARE}(\sigma)+b_s^2 m^2_{\rm BARE}(\sigma')$$
$$-\sqrt{2}a_s b_s(m^2_{\rm BARE}(\sigma)-m^2_{\rm BARE}(\sigma'))],$$

$$g_\eta^{(4)}=\frac{2}{F_\pi}\left[\frac{a_s}{\sqrt{2}}g_{\sigma\eta\eta}+\frac{b_s}{\sqrt{2}}g_{\sigma'\eta\eta}+\frac{2}{F_\pi}a_p^2(m^2_{\rm BARE}(a_0)-m_\eta^2)\right].\tag{A9}$$

Finally, the tree-level partial wave amplitudes for πK and $\pi\eta$ scattering are

$$T^{1/2}_{0tree}=\rho(s)\left[-2g_K^{(4)}+g^2_{\kappa K\pi}\left[-\frac{1}{4q^2}\ln\left(\frac{B_K+1}{B_K-1}\right)+\frac{3}{m^2_{\rm BARE}(\kappa)-s}\right]+\frac{1}{2q^2}g_{\sigma\pi\pi}g_{\sigma KK}\ln\left(\frac{m^2_{\rm BARE}(\sigma)+4q^2}{m^2_{\rm BARE}(\sigma)}\right)\right.$$
$$\left.+\frac{1}{2q^2}g_{\sigma'\pi\pi}g_{\sigma' KK}\ln\left(\frac{m^2_{\rm BARE}(\sigma')+4q^2}{m^2_{\rm BARE}(\sigma')}\right)\right]\tag{A10}$$

and

$$T^1_{0tree}=\rho(s)\left[-2g_\eta^{(4)}+g^2_{a_0\pi\eta}\left[\frac{1}{2q^2}\ln\left(\frac{B_\eta+1}{B_\eta-1}\right)+\frac{2}{m^2_{\rm BARE}(a_0)-s}\right]+\frac{1}{2q^2}g_{\sigma\pi\pi}g_{\sigma\eta\eta}\ln\left(1+\frac{4q^2}{m^2_{\rm BARE}(\sigma)}\right)\right.$$
$$\left.+\frac{1}{2q^2}g_{\sigma'\pi\pi}g_{\sigma'\eta\eta}\ln\left(1+\frac{4q^2}{m^2_{\rm BARE}(\sigma')}\right)\right],\tag{A11}$$

where $q(s)$ and $\rho(s)$ for each case are given by Eqs. (2.7) and (2.6) respectively. Furthermore

$$B_K=\frac{1}{2q^2}[m^2_{\rm BARE}(\kappa)-m_\pi^2-m_K^2+2\sqrt{(m_\pi^2+q^2)(m_K^2+q^2)}]\tag{A12}$$

and

$$B_\eta=\frac{1}{2q^2}[m^2_{\rm BARE}(a_0)-m_\pi^2-m_\eta^2+2\sqrt{(m_\pi^2+q^2)(m_\eta^2+q^2)}].\tag{A13}$$

[1] E. van Beveren, T.A. Rijken, K. Metzger, C. Dullemond, G. Rupp, and J.E. Ribeiro, Z. Phys. C **30**, 615 (1986); E. van Beveren and G. Rupp, Eur. Phys. J. C **10**, 469 (1999); **11**, 717 (1999); see also J.J. de Swart, P.M.M. Maessen, and T.A. Rijken, U.S./Japan Seminar on the YN Interaction, Maui, 1993 [Nijmegen report THEF-NYM 9403].

[2] D. Morgan and M. Pennington, Phys. Rev. D **48**, 1185 (1993).

[3] A.A. Bolokhov, A.N. Manashov, M.V. Polyakov, and V.V. Vereshagin, Phys. Rev. D **48**, 3090 (1993); see also V.A. Andrianov and A.N. Manashov, Mod. Phys. Lett. A **8**, 2199 (1993). Extension of this string-like approach to the πK case has been made in V.V. Vereshagin, Phys. Rev. D **55**, 5349 (1997), and very recently in A.V. Vereshagin and V.V. Vereshagin, *ibid.* **59**, 016002 (1999), which is consistent with a light κ state.

[4] N.N. Achasov and G.N. Shestakov, Phys. Rev. D **49**, 5779 (1994).

[5] R. Kamínski, L. Leśniak, and J. P. Maillet, Phys. Rev. D **50**, 3145 (1994).

[6] F. Sannino and J. Schechter, Phys. Rev. D **52**, 96 (1995).

[7] N.A. Törnqvist, Z. Phys. C **68**, 647 (1995), and references therein. In addition see N.A. Törnqvist and M. Roos, Phys.

Rev. Lett. **76**, 1575 (1996); N.A. Törnqvist, hep-ph/9711483; Phys. Lett. B **426**, 105 (1998).
[8] R. Delbourgo and M.D. Scadron, Mod. Phys. Lett. A **10**, 251 (1995); see also D. Atkinson, M. Harada, and A.I. Sanda, Phys. Rev. D **46**, 3884 (1992).
[9] G. Janssen, B.C. Pearce, K. Holinde, and J. Speth, Phys. Rev. D **52**, 2690 (1995).
[10] M. Svec, Phys. Rev. D **53**, 2343 (1996).
[11] S. Ishida, M.Y. Ishida, H. Takahashi, T. Ishida, K. Takamatsu, and T. Tsuru, Prog. Theor. Phys. **95**, 745 (1996); S. Ishida, M. Ishida, T. Ishida, K. Takamatsu, and T. Tsuru, *ibid.* **98**, 621 (1997); see also M. Ishida and S. Ishida, talk given at 7th International Conference on Hadron Spectroscopy (Hadron 97), Upton, NY, 1997, hep-ph/9712231.
[12] M. Harada, F. Sannino, and J. Schechter, Phys. Rev. D **54**, 1991 (1996).
[13] M. Harada, F. Sannino, and J. Schechter, Phys. Rev. Lett. **78**, 1603 (1997).
[14] D. Black, A.H. Fariborz, F. Sannino, and J. Schechter, Phys. Rev. D **58**, 054012 (1998).
[15] D. Black, A.H. Fariborz, F. Sannino, and J. Schechter, Phys. Rev. D **59**, 074026 (1999).
[16] J.A. Oller, E. Oset, and J.R. Pelaez, Phys. Rev. Lett. **80**, 3452 (1998); J.A. Oller and E. Oset, Phys. Rev. D **60**, 074023 (1999); M. Jamin, J.A. Oller, and A. Pich, Nucl. Phys. **B587**, 331 (2000); see also K. Igi and K. Hikasa, Phys. Rev. D **59**, 034005 (1999).
[17] A.V. Anisovich and A.V. Sarantsev, Phys. Lett. B **413**, 137 (1997).
[18] V. Elias, A.H. Fariborz, Fang Shi, and T.G. Steele, Nucl. Phys. **A633**, 279 (1998).
[19] V. Dmitrasinović, Phys. Rev. C **53**, 1383 (1996).
[20] P. Minkowski and W. Ochs, Eur. Phys. J. C **9**, 283 (1999).
[21] S. Godfrey and J. Napolitano, Rev. Mod. Phys. **71**, 1411 (1999).
[22] L. Burakovsky and T. Goldman, Phys. Rev. D **57**, 2879 (1998).
[23] D. Black, A. H. Fariborz, and J. Schechter, Phys. Rev. D **59**, 074026 (1999).
[24] D. Black, A. H. Fariborz, and J. Schechter, Phys. Rev. D **61**, 074030 (2000); see also V. Bernard, N. Kaiser, and U.-G. Meissner, *ibid.* **44**, 3698 (1991); A. H. Fariborz and J. Schechter, *ibid.* **60**, 034002 (1999).
[25] D. Black, A. H. Fariborz, and J. Schechter, Phys. Rev. D **61**, 074001 (2000).
[26] L. Celenza, S.-f. Gao, B. Huang, and C.M. Shakin, Phys. Rev. C **61**, 035201 (2000).
[27] An up to date summary of the status of the light scalar mesons is available in ''Possible Existence of the σ-meson and its Implications to Hadron Physics,'' KEK Proceedings 2000-4, Soryushiron Kenkyan 102, No. 5, 2001.
[28] J. Gasser and H. Leutwyler, Ann. Phys. (N.Y.) **158**, 142 (1984); Nucl. Phys. **B250**, 465 (1985). A more recent review is given by U.-G. Meissner, Rep. Prog. Phys. **56**, 903 (1993).
[29] E. Witten, Nucl. Phys. **B160**, 57 (1979); see also S. Coleman, *Aspects of Symmetry* (Cambridge University Press, Cambridge, England, 1985); the original suggestion is given in G. 't Hooft, Nucl. Phys. **B72**, 461 (1974).
[30] See Refs. [1–27] above.
[31] M. Gell-Mann and M. Lévy, Nuovo Cimento **16**, 705 (1960).
[32] J. Cronin, Phys. Rev. **161**, 1483 (1967); S. Weinberg, Phys. Rev. Lett. **18**, 188 (1967).
[33] T. Hatsuda, T. Kunihiro, and H. Shimizu, Phys. Rev. Lett. **82**, 2840 (1999); S. Chiku and T. Hatsuda, Phys. Rev. D **58**, 076001 (1998).
[34] See also L.H. Chan and R.W. Haymaker, Phys. Rev. **7**, 402 (1973); **10**, 4170 (1974).
[35] See, for example, S.U. Chung *et al.*, Ann. Phys. (Leipzig) **4**, 404 (1995); see also T.N. Truong, Phys. Rev. Lett. **67**, 2260 (1991).
[36] M. Lévy, Nuovo Cimento A **52**, 23 (1967); see S. Gasiorowicz and D.A. Geffen, Rev. Mod. Phys. **41**, 531 (1969), for a review which contains a large bibliography.
[37] J. Schechter and Y. Ueda, Phys. Rev. D **3**, 2874 (1971); **8**, 987(E) (1973); see also J. Schechter and Y. Ueda, *ibid.* **3**, 168 (1971).
[38] H. Gomm, P. Jain, R. Johnson, and J. Schechter, Phys. Rev. D **33**, 801 (1986).
[39] V. Mirelli and J. Schechter, Phys. Rev. D **15**, 1361 (1977).
[40] J. Schechter and Y. Ueda, Phys. Rev. D **4**, 733 (1971).
[41] W. Hudnall and J. Schechter, Phys. Rev. D **9**, 2111 (1974); see footnote in Sec. I of the present paper for corrections of typographical errors.
[42] S. Weinberg, Phys. Rev. Lett. **17**, 616 (1966).
[43] C. Callan, S. Coleman, J. Wess, and B. Zumino, Phys. Rev. **177**, 2247 (1969).
[44] E.A. Alekseeva *et al.*, Zh. Éksp. Teor. Fiz. **82**, 1007 (1982) [Sov. Phys. JETP **55**, 591 (1982)]; G. Grayer *et al.*, Nucl. Phys. **B75**, 189 (1974).
[45] D. Aston *et al.*, Nucl. Phys. **B296**, 493 (1988).
[46] Particle Data Group, D. Groom *et al.*, Eur. Phys. J. C **15**, 1 (2000).
[47] S. Cherry and M. Pennington, hep-ph/0005208.
[48] D. Black, A.H. Fariborz, and J. Schechter, hep-ph/0008246.
[49] U.G. Meissner and J.A. Oller, Phys. Lett. B **500**, 263 (2001); Phys. Rev. D **64**, 014006 (2001).
[50] N. Isgur and J. Weinstein, Phys. Rev. Lett. **48**, 659 (1982); Phys. Rev. D **27**, 588 (1983); see also F.E. Close, N. Isgur, and S. Kumano, Nucl. Phys. **B389**, 513 (1993).
[51] R.L. Jaffe, Phys. Rev. D **15**, 267 (1977); see also N. Achasov and V.N. Ivanchenko, Nucl. Phys. **B315**, 465 (1989); M.N. Achasov *et al.*, Phys. Lett. B **440**, 442 (1998).
[52] S. Okubo, Phys. Lett. **5**, 165 (1963).